Chiral symmetry and deconfinement signatures within PHSD and PHQMD models

Elena Bratkovskaya

(GSI, Darmstadt & Uni. Frankfurt)

for the PHSD/PHQMD group

CBM symposium & CBM Collaboration meeting

GSI, Darmstadt, October 03, 2018.

The ‚holy grail‘ of heavy-ion physics:

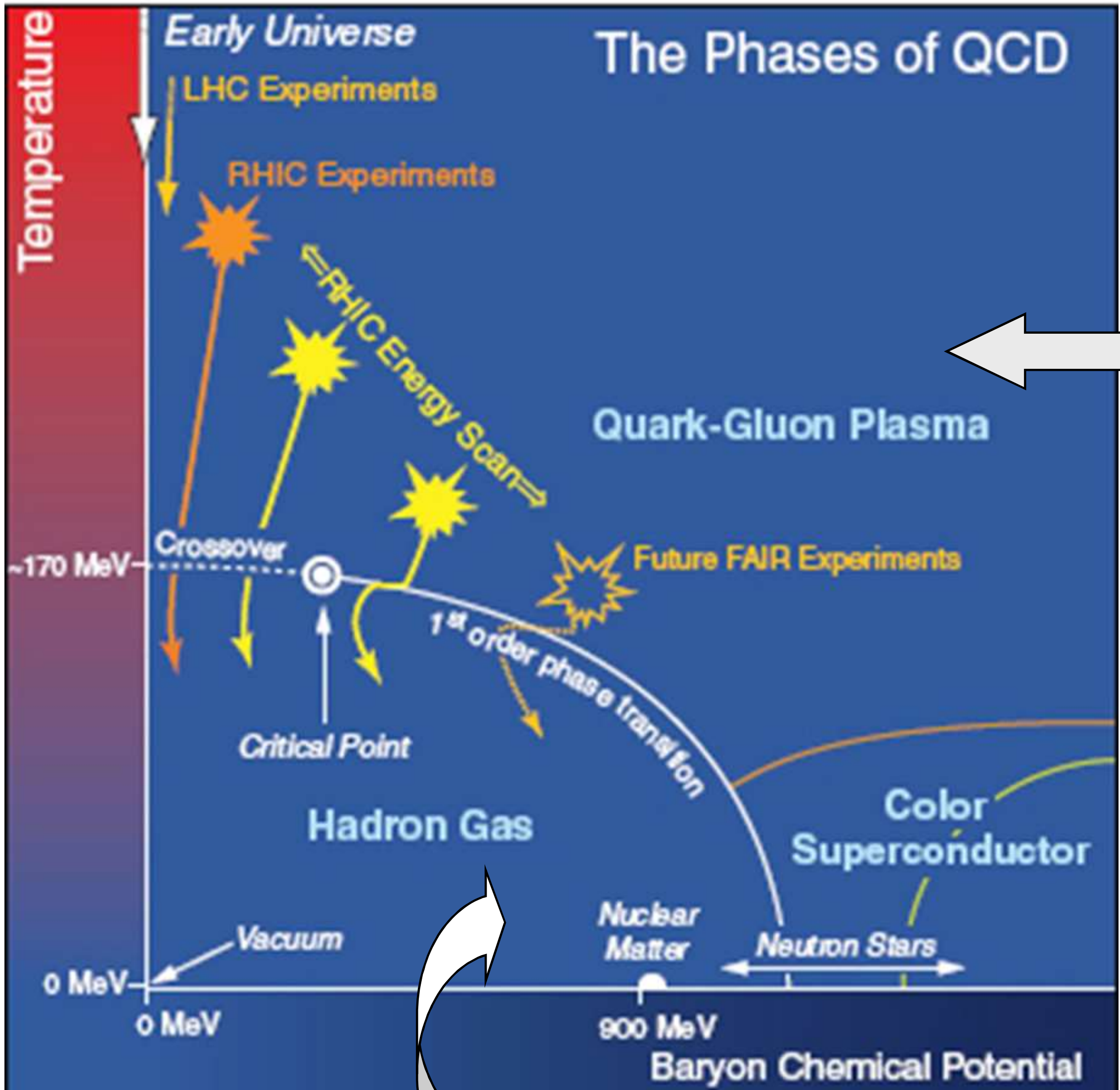

The phase diagram of QCD

- Study of the phase transition from hadronic to partonic matter – Quark-Gluon-Plasma

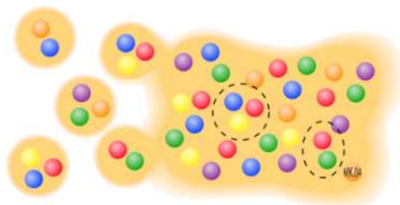

- Search for the critical point
- Search for signatures of chiral symmetry restoration
- Study of the in-medium properties of hadrons at high baryon density and temperature

Theory: Information from lattice QCD

I. deconfinement phase transition with increasing temperature + **II. chiral symmetry restoration with increasing temperature**

lQCD BMW collaboration: $\mu_q=0$

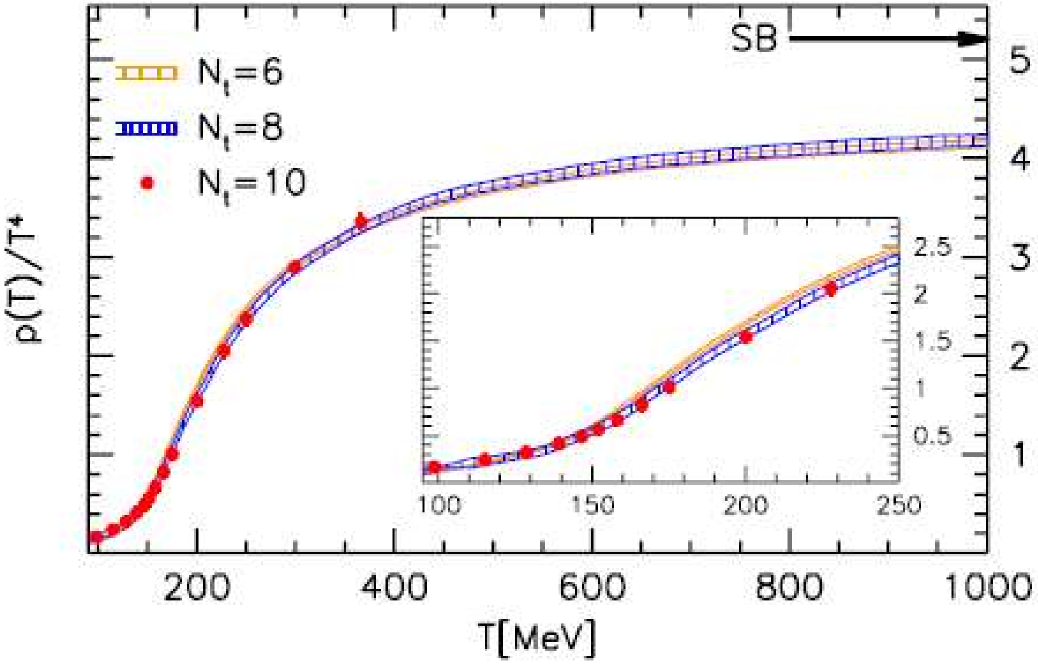

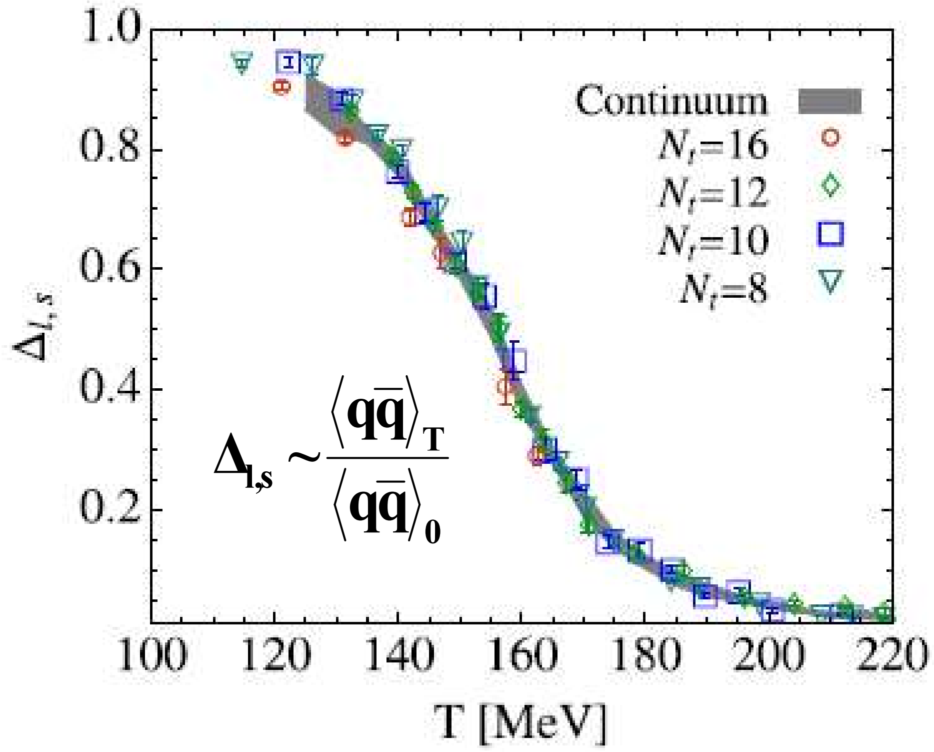

- **Crossover: hadron gas → QGP**
- **Scalar quark condensate $\langle q\bar{q}\rangle$ is viewed as an order parameter for the restoration of chiral symmetry:**

$$<\bar{q}q>= \begin{cases} \neq 0 & \text{chiral non-symmetric phase;} \\ = 0 & \text{chiral symmetric phase.} \end{cases}$$

→ **both transitions occur at about the same temperature T_C for low chemical potentials**

Signals for the phase transition

Hadron-string transport models (HSD, UrQMD) versus observables at ~ 2000

❑ ‚horn' in K^+/π^+

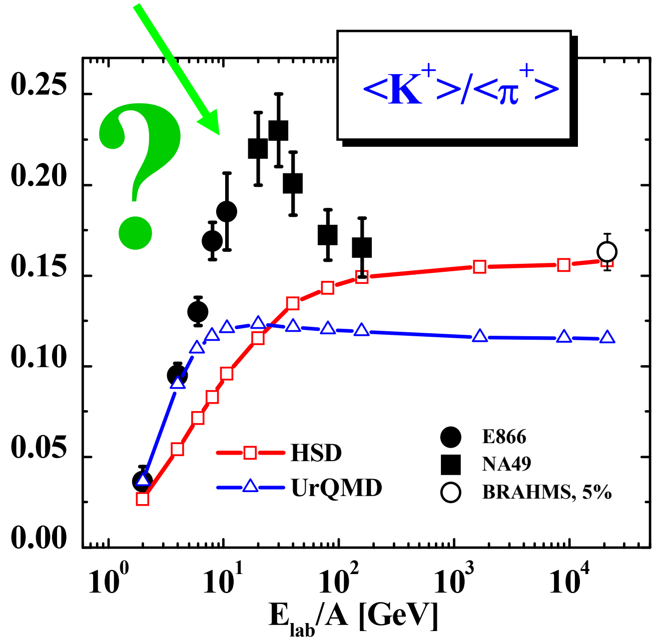

❑ ‚step' in slope T

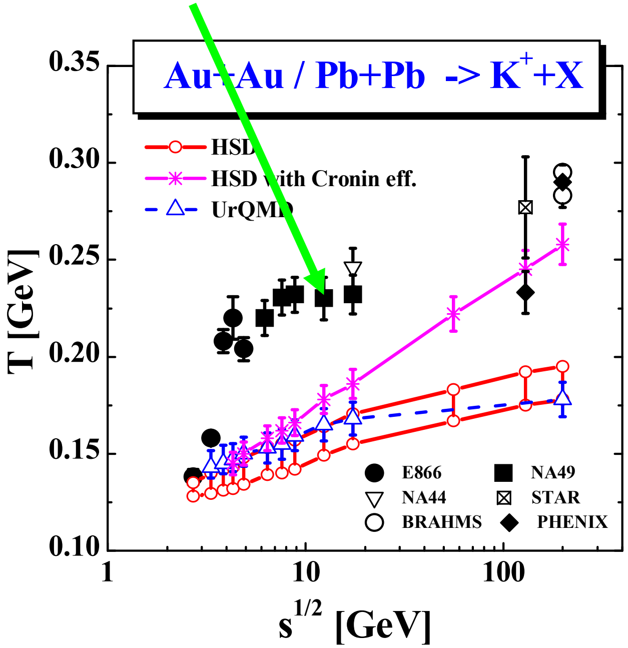

❑ elliptic flow v_2

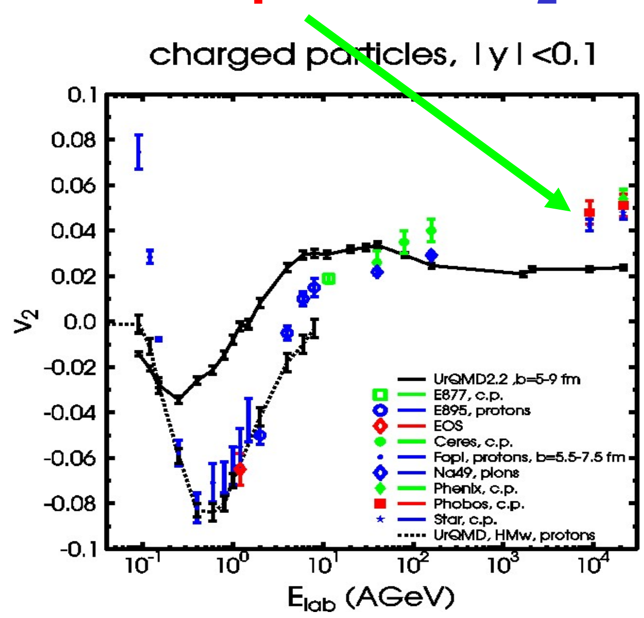

Exp. data are not reproduced in terms of the hadron-string picture
➔ evidence for partonic degrees of freedom + ... ?!

NA49: PRC66 (2002) 054902

HSD, UrQMD: PRC 69 (2004) 032302

Dynamical description of heavy-ion collisions

The goal:
to study the properties of strongly interacting matter under extreme conditions from a microscopic point of view

Realization:
to develop a dynamical many-body transport approach
1) applicable for strongly interacting systems, which includes:
2) phase transition from hadronic matter to QGP
3) chiral symmetry restoration

2004

2018

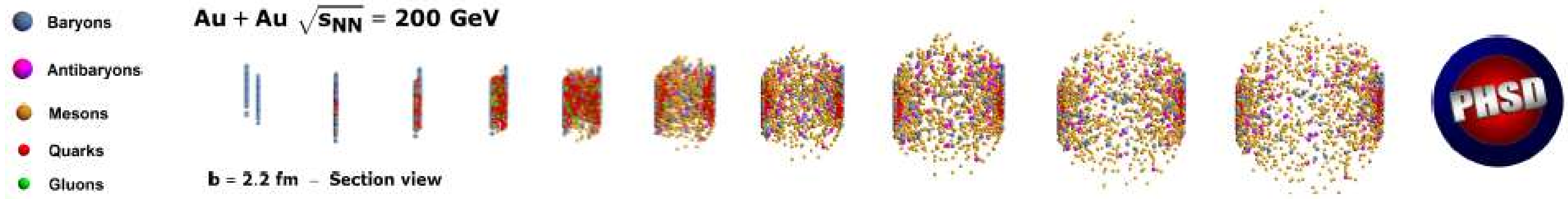

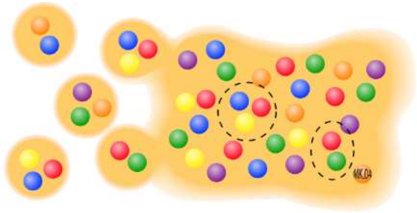

Degrees-of-freedom of QGP

❖ lQCD gives QGP EoS at finite μ_B

! need to be interpreted in terms of degrees-of-freedom

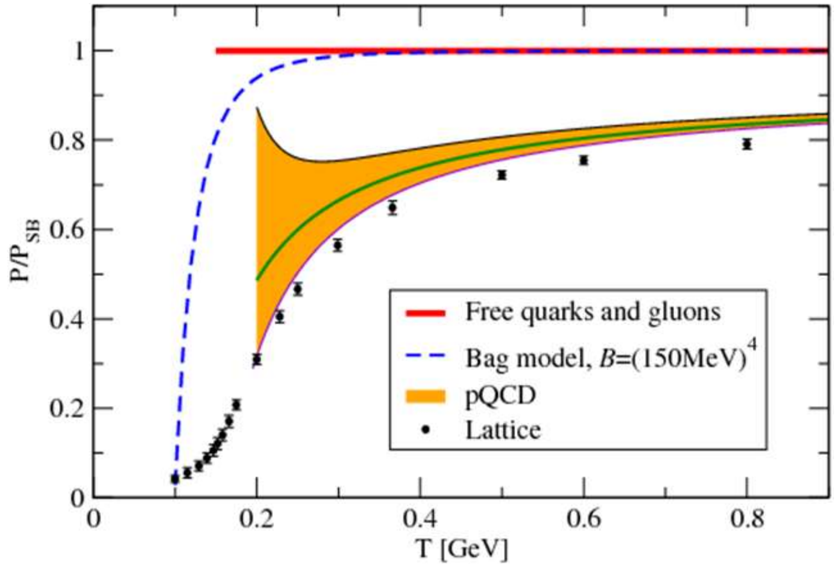

Non-perturbative QCD ← pQCD

Thermal QCD
= QCD at high parton densities:

- strongly interacting system
- massive quarks and gluons

➔ quasiparticles
= effective degrees-of-freedom

pQCD:

- weakly interacting system
- massless quarks and gluons

❖ How to learn about degrees-of-freedom of QGP ? ➔ HIC experiments

Dynamical QuasiParticle Model (DQPM) - Basic ideas:

DQPM describes QCD properties in terms of ‚resummed' single-particle Green's functions (propagators) – in the sense of a two-particle irreducible (2PI) approach:

gluon propagator: $\Delta^{-1} = P^2 - \Pi$ & quark propagator $S_q^{-1} = P^2 - \Sigma_q$

gluon self-energy: $\Pi = M_g^2 - i2\gamma_g\omega$ & quark self-energy: $\Sigma_q = M_q^2 - i2\gamma_q\omega$

(scalar approximation)

- the resummed properties are specified by complex (retarded) self-energies:
- the real part of self-energies (Σ_q, Π) describes a dynamically generated mass (M_q,M_g);
- the imaginary part describes the interaction width of partons (γ_q, γ_g)
- Spectral functions : $A_q \sim Im S_q^{ret}, \quad A_g \sim Im\Delta^{ret}$

- Entropy density of interacting bosons and fermions in the quasiparticle limit (2PI) (G. Baym 1998):

QGP

$$s^{dqp} = -d_g \int \frac{d\omega}{2\pi} \frac{d^3p}{(2\pi)^3} \frac{\partial n_B}{\partial T} \left(\mathrm{Im}\ln(-\Delta^{-1}) + \mathrm{Im}\,\Pi\,\mathrm{Re}\,\Delta\right) \quad \text{gluons}$$

$$- d_q \int \frac{d\omega}{2\pi} \frac{d^3p}{(2\pi)^3} \frac{\partial n_F((\omega-\mu_q)/T)}{\partial T} \left(\mathrm{Im}\ln(-S_q^{-1}) + \mathrm{Im}\,\Sigma_q\,\mathrm{Re}\,S_q\right) \quad \text{quarks}$$

$$- d_{\bar q} \int \frac{d\omega}{2\pi} \frac{d^3p}{(2\pi)^3} \frac{\partial n_F((\omega+\mu_q)/T)}{\partial T} \left(\mathrm{Im}\ln(-S_{\bar q}^{-1}) + \mathrm{Im}\,\Sigma_{\bar q}\,\mathrm{Re}\,S_{\bar q}\right) \quad \text{antiquarks}$$

A. Peshier, W. Cassing, PRL 94 (2005) 172301; Cassing, NPA 791 (2007) 365: NPA 793 (2007)

DQPM(T): properties of quasiparticles

Properties of **interacting quasi-particles:**
massive quarks and gluons (g, q, q_{bar})
with **Lorentzian spectral functions :**

$$A(\omega,\mathbf{p}) = \frac{\gamma}{E}\left(\frac{1}{(\omega-E)^2+\gamma^2} - \frac{1}{(\omega+E)^2+\gamma^2}\right)$$

$$E^2 = p^2 + M^2 - \gamma^2$$

- Modeling of the quark/gluon masses and widths → HTL limit at high T

m~gT

masses: $m_g^2 = \frac{g^2}{6}\left(N_c + \frac{1}{2}N_f\right)T^2\,, \qquad m_q^2 = g^2\frac{N_c^2-1}{8N_c}T^2$

widths: $\gamma_g = \frac{1}{3}N_c\frac{g^2T}{8\pi}\ln\left(\frac{2c}{g^2}+1\right)\,, \quad \gamma_q = \frac{1}{3}\frac{N_c^2-1}{2N_c}\frac{g^2T}{8\pi}\ln\left(\frac{2c}{g^2}+1\right)$

- **running coupling** (pure glue):

$$\alpha_s(T) = \frac{g^2(T)}{4\pi} = \frac{12\pi}{(11N_c - 2N_f)\ln[\lambda^2(T/T_c - T_s/T_c)^2]}$$

- ❑ **fit to lattice (lQCD) results** (e.g. entropy density)

  with 3 parameters: T_s/T_c=0.46; c=28.8; λ=2.42 (for pure glue N_f=0)

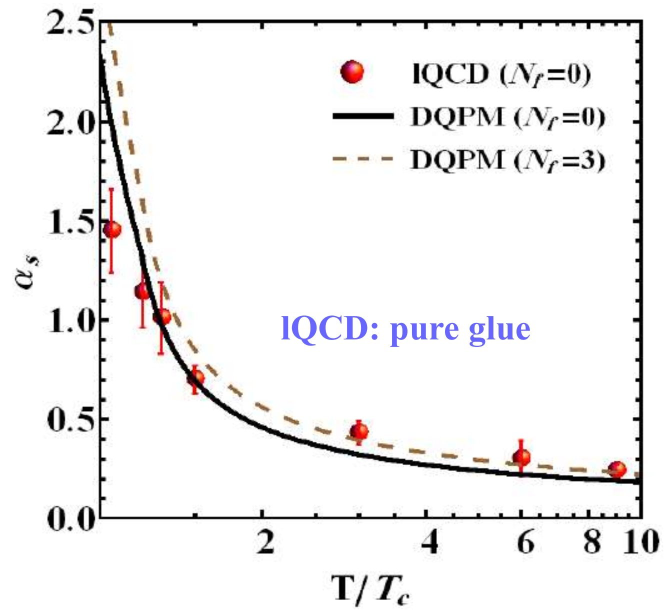

Peshier, Cassing, PRL 94 (2005) 172301;
Cassing, NPA 791 (2007) 365: NPA 793 (2007)

DQPM at finite T and μ_q=0

- fit to lattice (lQCD) results
  - * BMW lQCD data S. Borsanyi et al., JHEP 1009 (2010) 073

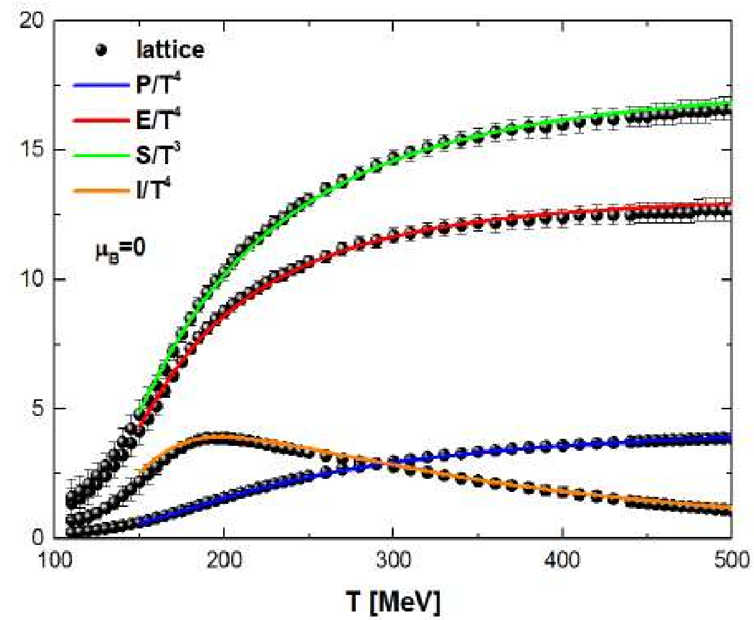

➔ Quasiparticle properties:
- large width and mass for gluons and quarks

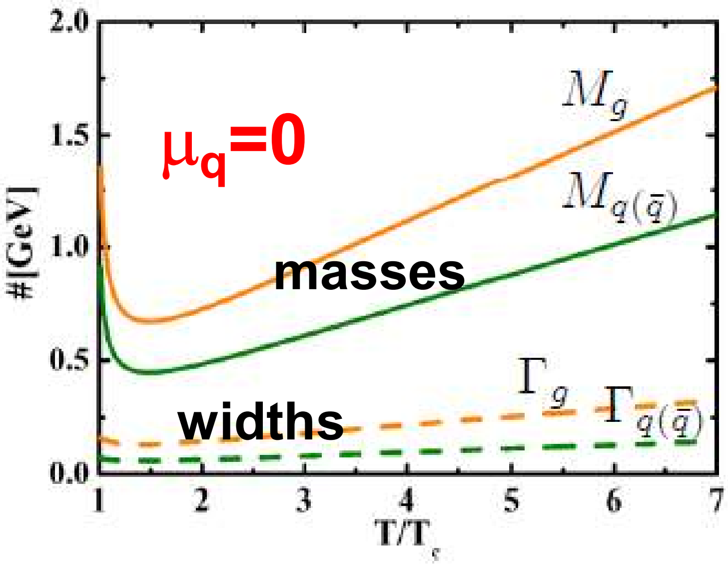

M~gT

T_C=158 MeV
ε_C=0.5 GeV/fm³

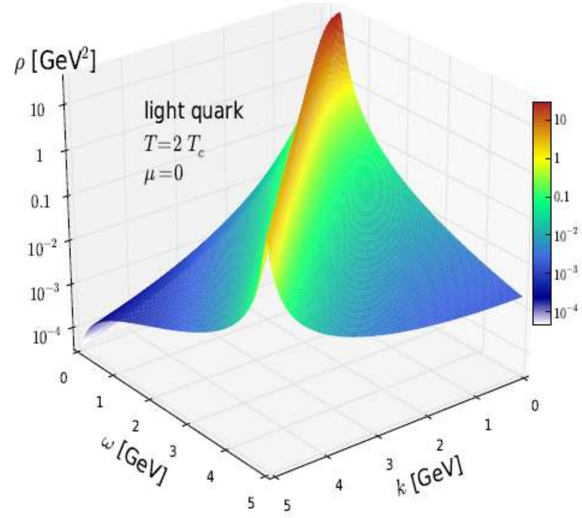

DQPM
- matches well lattice QCD
- provides mean-fields (1PI) for gluons and quarks – from space-like part of $T_{\mu\nu}$ as well as effective 2-body interactions (2PI)
- gives transition rates for the formation of hadrons

➔ microscopic dynamical transport approach PHSD

Peshier, Cassing, PRL 94 (2005) 172301; Cassing, NPA 791 (2007) 365: NPA 793 (2007)

Basic idea: off-shell PHSD approach

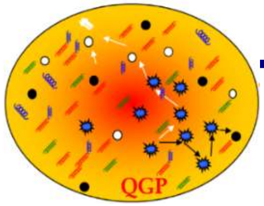

QGP in equilibrium

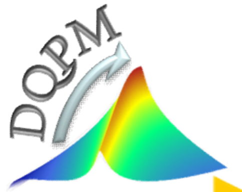

Dynamical QuasiParticle Model (DQPM):

fitted to → **lQCD**

Quasiparticle properties:
‚resummed' self-energies, propagators
➔ Calculation of cross sections

➔ **Calculation of transport coefficients in equilibrium** $\eta, \zeta, \sigma_0, ..$

controled by lQCD!

DQPM: consider the effects of the nonperturbative nature of the strongly interacting quark-gluon plasma (sQGP) constituents (vs. pQCD models)

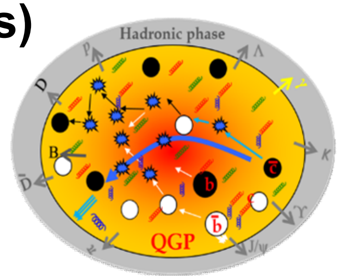

QGP out-of equilibrium ←→ HIC

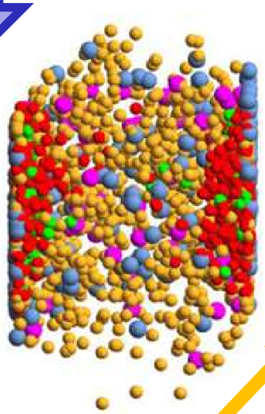

Parton-Hadron-String-Dynamics (PHSD)

controled by → **experimental data + lQCD**

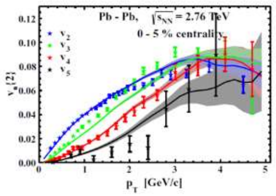

Partonic interactions → DQPM
hadronic interactions → hadron physics
*** In-medium hadronic interactions → many-body physics: G-matrix**

Parton-Hadron-String-Dynamics (PHSD)

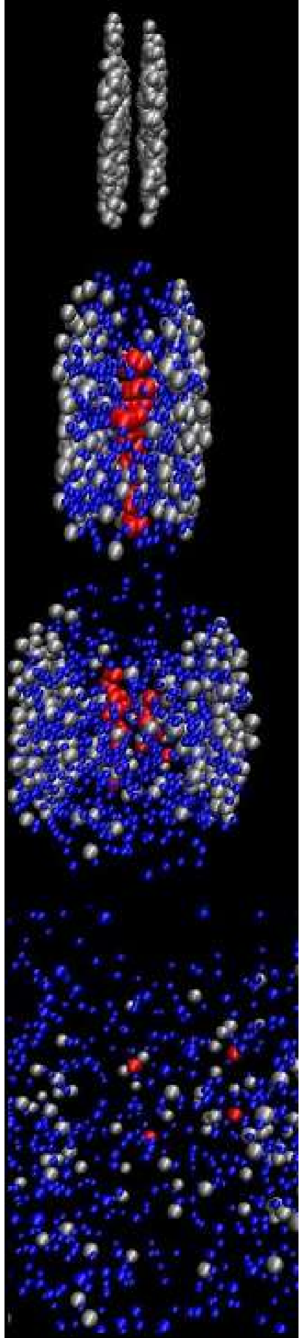

- **Initial A+A collisions :**
  N+N → string formation → decay to pre-hadrons

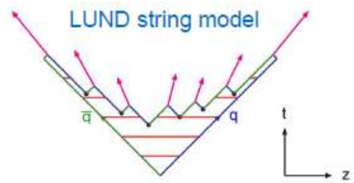

- **Formation of QGP stage if $\varepsilon > \varepsilon_{critical}$:**
  dissolution of pre-hadrons → (DQPM) →
  → massive quarks/gluons + mean-field potential U_q

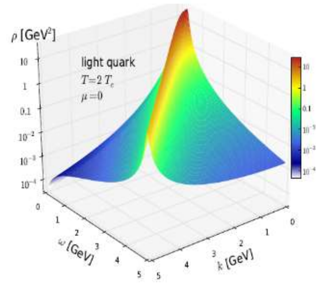

- **Partonic stage – QGP :**
  based on the Dynamical Quasi-Particle Model (DQPM)

  - (quasi-) elastic collisions:

$$q+q \to q+q \qquad g+q \to g+q$$
$$q+\bar{q} \to q+\bar{q} \qquad g+\bar{q} \to g+\bar{q}$$
$$\bar{q}+\bar{q} \to \bar{q}+\bar{q} \qquad g+g \to g+g$$

  - inelastic collisions:

$$q+\bar{q} \to g \qquad q+\bar{q} \to g+g$$
$$g \to q+\bar{q} \qquad g \to g+g$$

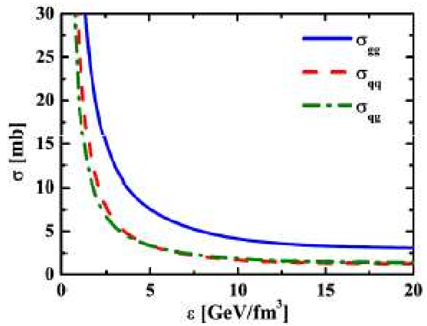

- **Hadronization (based on DQPM):**

$$g \to q+\bar{q}, \qquad q+\bar{q} \leftrightarrow meson \ (or\ 'string')$$
$$q+q+q \leftrightarrow baryon \ (or\ 'string')$$

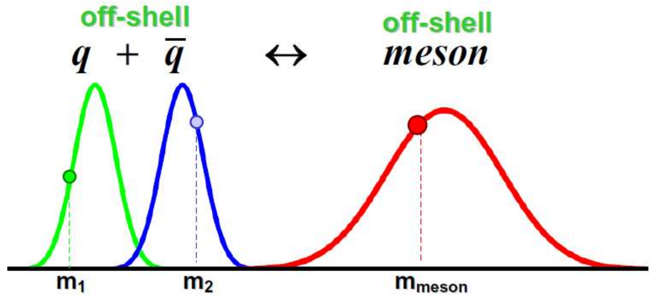

- **Hadronic phase: hadron-hadron interactions – off-shell HSD**

W. Cassing, E. Bratkovskaya, PRC 78 (2008) 034919; NPA831 (2009) 215; W. Cassing, EPJ ST 168 (2009) 3

QGP in equilibrium: Transport properties at finite (T, μ_q): η/s

Infinite hot/dense matter = PHSD in a box:

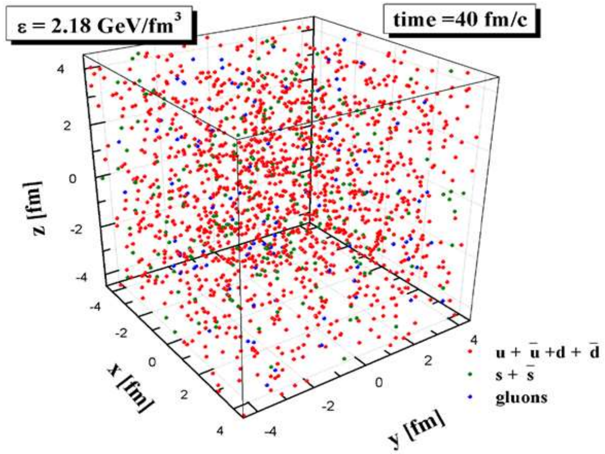

Shear viscosity η/s at finite T

PHSD: V. Ozvenchuk et al., PRC 87 (2013) 064903

Hydro: Bayesian analysis, S. Bass et al. ,1704.07671

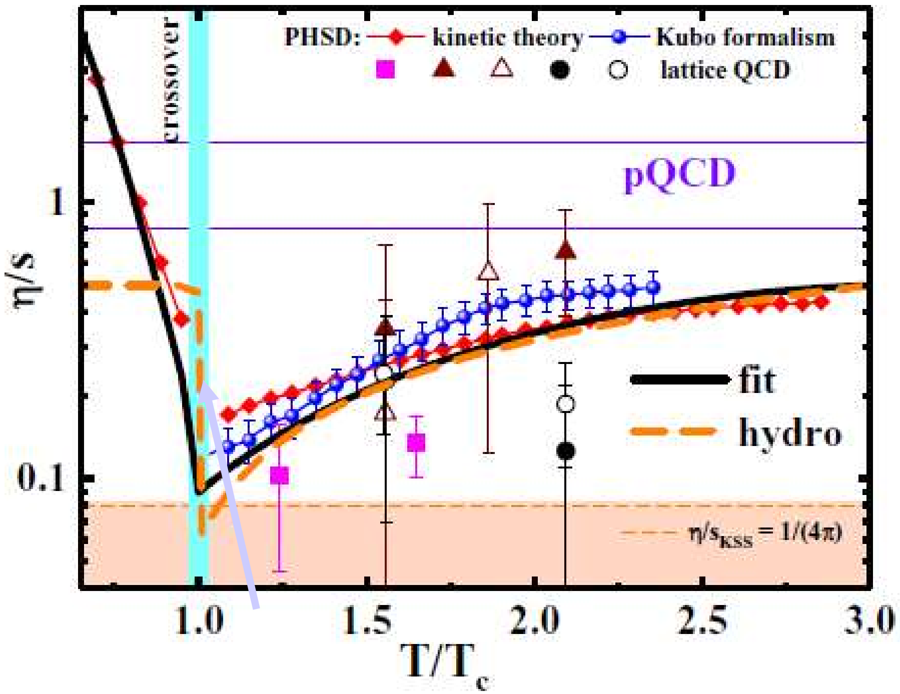

Shear viscosity η/s at finite (T, μ_q)

lQCD:
$$\frac{T_c(\mu_q)}{T_c(\mu_q=0)} = \sqrt{1-\alpha\,\mu_q^2} \approx 1 - \alpha/2\,\mu_q^2 + \cdots$$

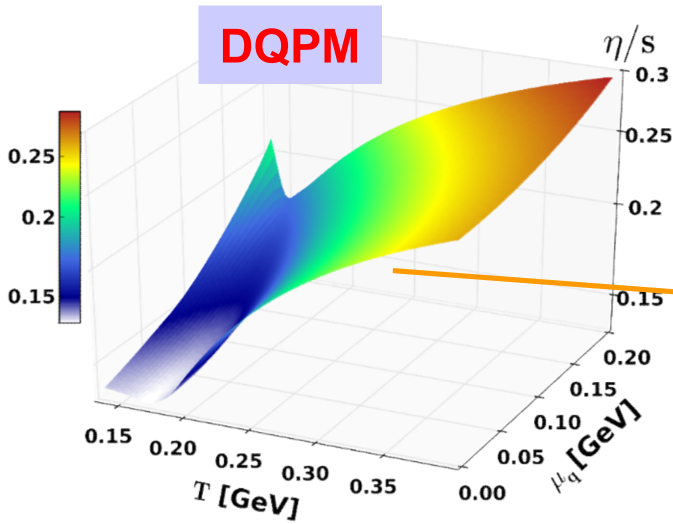

QGP in PHSD = strongly-interacting liquid-like system

η/s: μ_q=0 ➔ finite μ_q: smooth increase as a function of (T, μ_q)

Review: H. Berrehrah et al. Int.J.Mod.Phys. E25 (2016) 1642003

Traces of the QGP in observables in high energy heavy-ion collisions

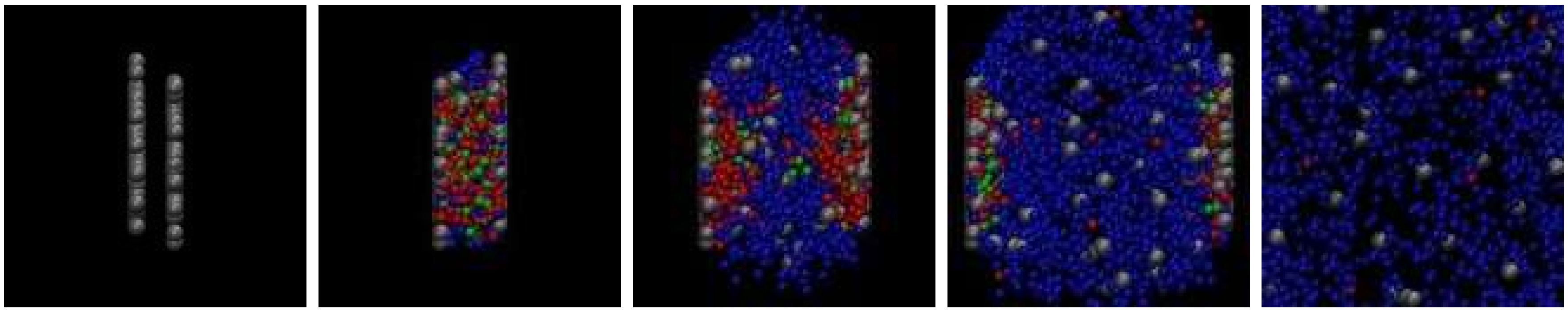

http://theory.gsi.de/~ebratkov/phsd-project/PHSD/index1.html

Partonic energy fraction in central A+A

Time evolution of the partonic energy fraction vs energy

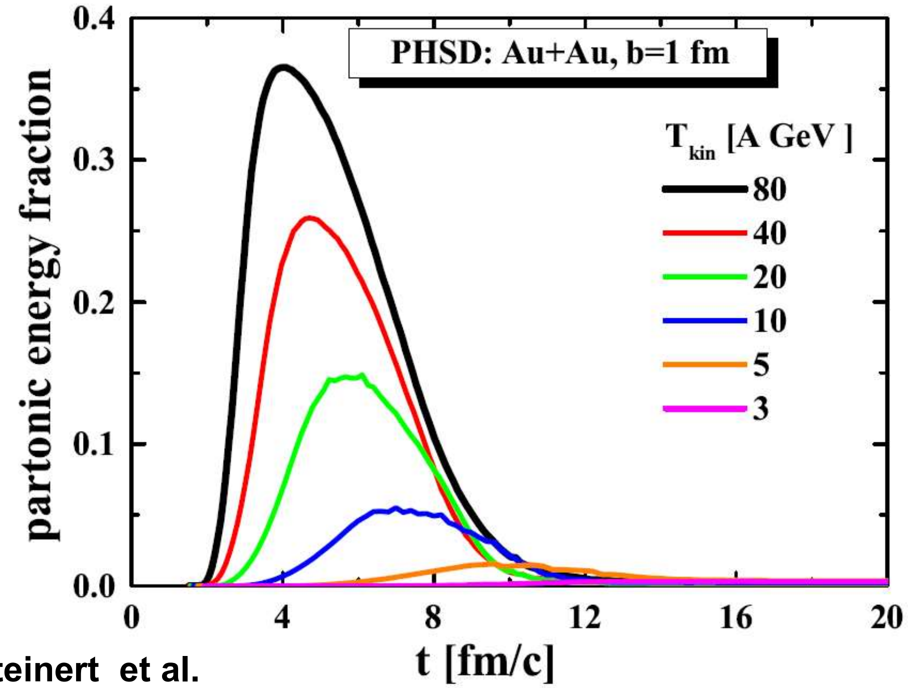

T. Steinert et al.

Au+Au, midrapidity

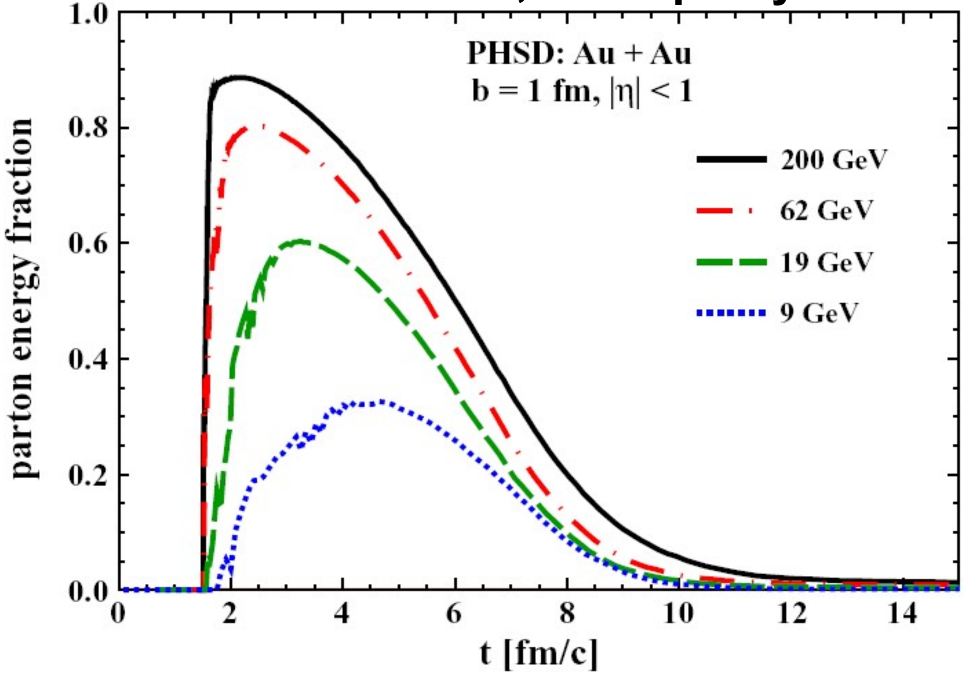

- Strong increase of partonic phase with energy from AGS to RHIC

- SPS: Pb+Pb, 160 A GeV: only about 40% of the converted energy goes to partons; the rest is contained in the large hadronic corona and leading partons
- RHIC: Au+Au, 21.3 A TeV: up to 90% - QGP

W. Cassing & E. Bratkovskaya, NPA 831 (2009) 215
V. Konchakovski et al., Phys. Rev. C 85 (2012) 011902

Time evolution of particle density distribution

Example: dN/dxdz for Pb+Pb, 30 A GeV, b=1 fm, y=0

Baryons:

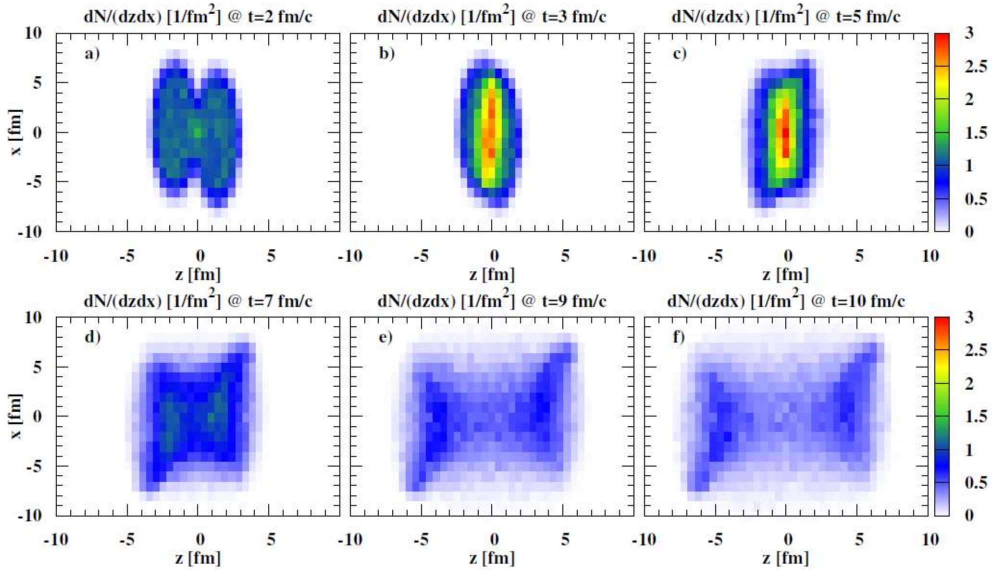

Partons:

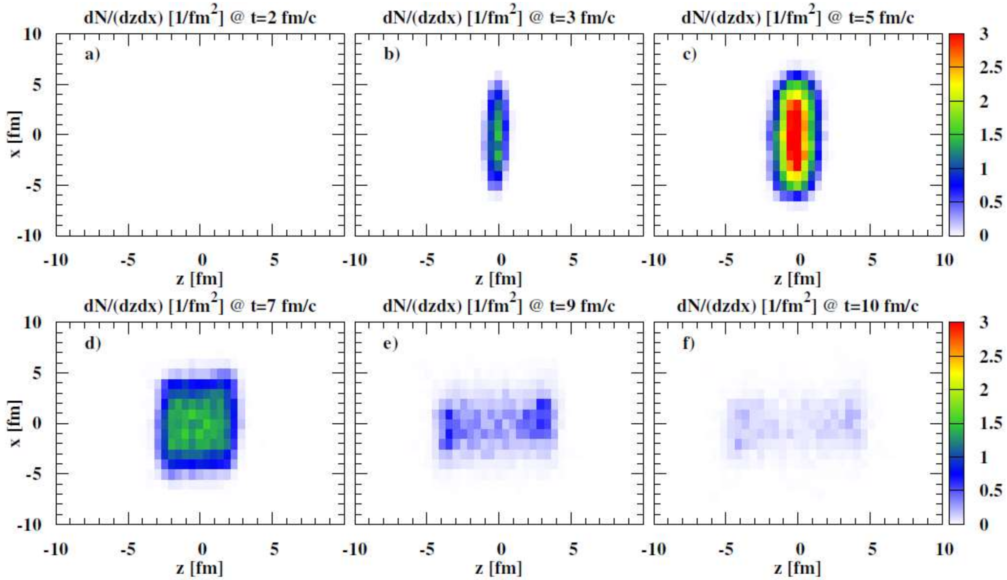

Mesons:

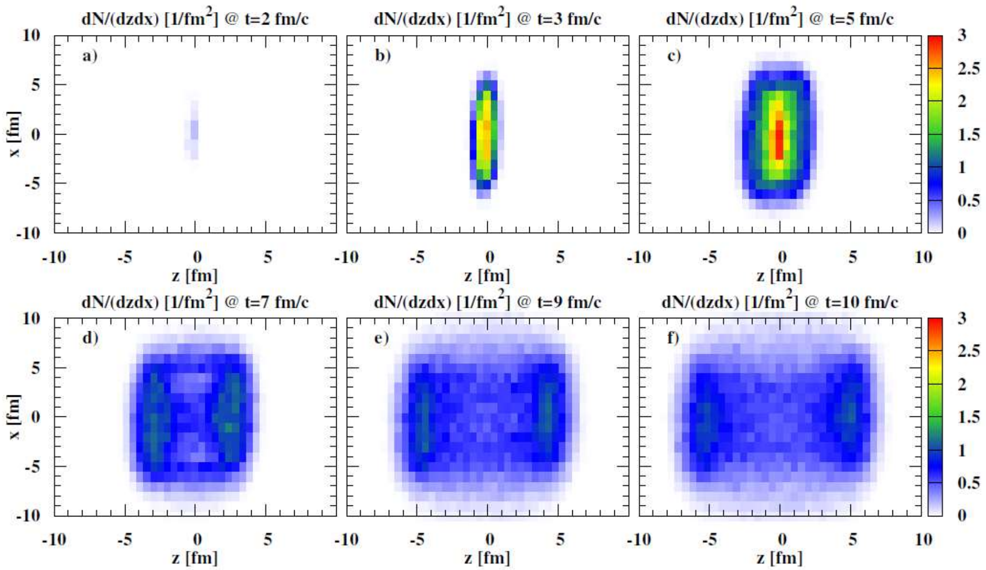

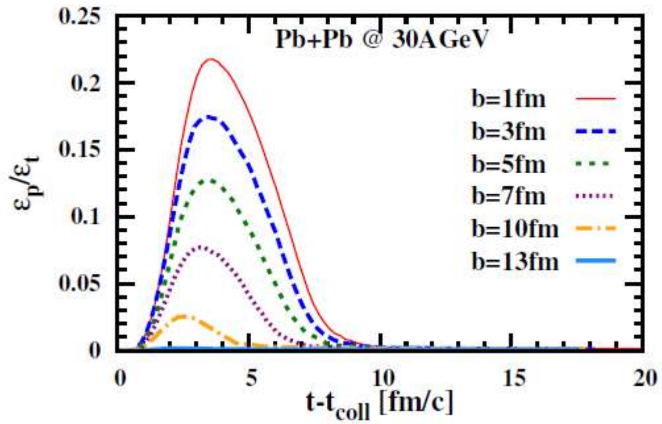

At central Pb+Pb at 30 AGeV the fraction of QGP < 20%

Problem: K^+/π^+ ‚horn' – 2015

PHSD: even when considering the creation of a QGP phase, the K^+/π^+ ‚horn' seen experimentally by NA49 and STAR at a bombarding energy ~30 A GeV (FAIR/NICA energies!) remains unexplained !

➔ The origin of 'horn' is not traced back to deconfinement ?!

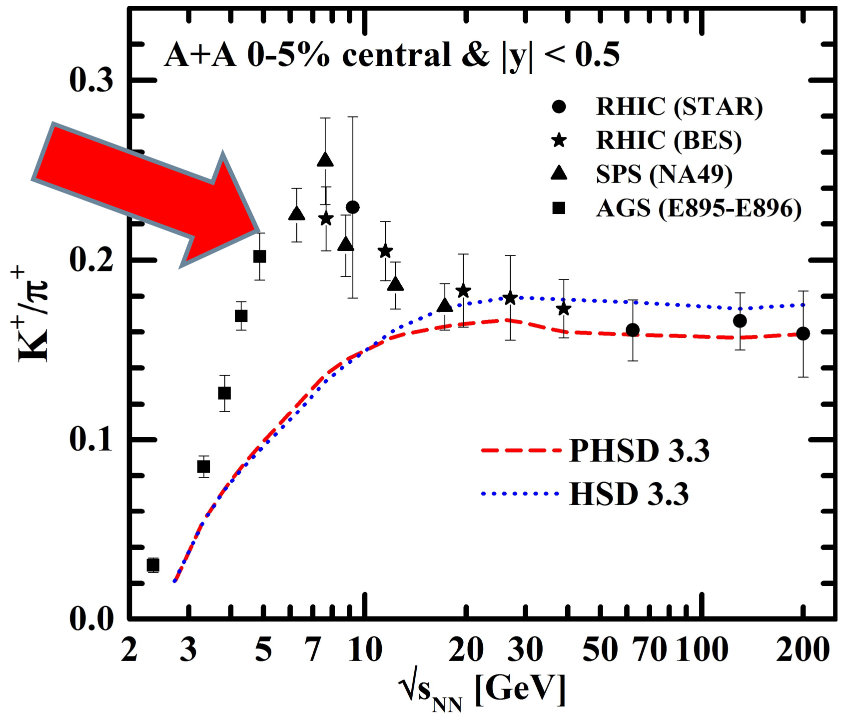

lQCD BMW collaboration:

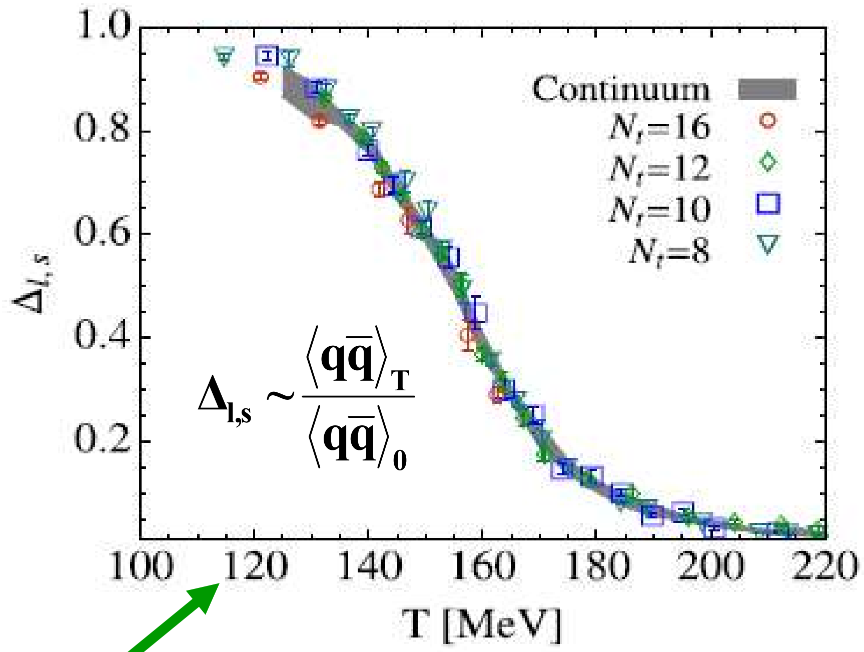

?

Can it be related to chiral symmetry restoration in the hadronic phase?!

W. Cassing, A. Palmese, P. Moreau, E.L. Bratkovskaya, PRC 93, 014902 (2016)

Chiral symmetry restoration via Schwinger mechanism

- **Initial stage of HIC: string formation**

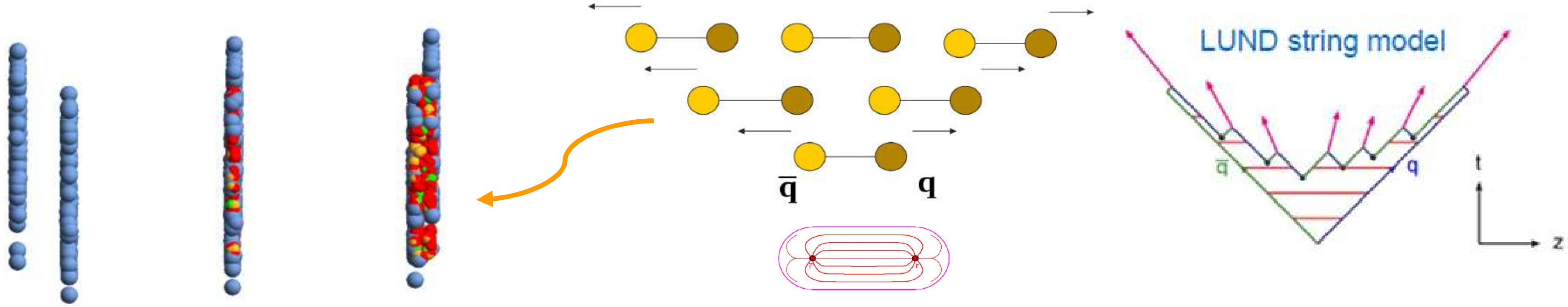

- **the ‚flavor chemistry' of the final hadrons in the PHSD is mainly defined by the LUND string model**

- **'quark flavor chemistry' in the LUND model is determined by the Schwinger-formula**

- **According to the Schwinger-formula, the probability to form a massive $s\bar{s}$ pair in a string-decay is suppressed in comparison to a light flavor pair $(u\bar{u}, d\bar{d})$:**

$$\frac{P(s\bar{s})}{P(u\bar{u})} = \frac{P(s\bar{s})}{P(d\bar{d})} = \gamma_S = \exp\left(-\pi \frac{m_S^2 - m_q^2}{2\kappa}\right)$$

with κ- string tension;
in vacuum: κ~0.9 GeV/fm=0.176GeV²

- **m_s, m_q (q=u,d) – constituent ('dressed') quark masses**

Dressing of the quark masses

- m_s, m_q (q=u,d) – constituent ('dressed') quark masses: 'dressing' of bare quark masses is due to the coupling to the scalar quark condensate $<q\bar{q}>$:

I. In vacuum (e.g. p+p collisions) :

$$m_q^V = m_q^0 - g_s <q\bar{q}>_V$$

$(V \equiv vacuum)$

bare quark masses:

$$m_u^0 = m_d^0 \approx 7 MeV, \; m_s^0 \approx 100 MeV$$

vacuum scalar quark condensate fixed from Gell-Mann-Oakes-Renner relation $f_\pi^2 m_\pi^2 = -\frac{1}{2}(m_u^0 + m_d^0) < \bar{q}q >_V$

$$\Rightarrow <q\bar{q}>_V \approx -3.2 fm^{-3}$$

→ Constituent quark masses in vacuum :

$$(m_q \equiv m_q^V) \quad m_u^V = m_d^V \approx 0.35 GeV, \quad m_s^V \approx 0.5 GeV$$

II. In medium (e.g. A+A collisions) :

In the presence of a hot and dense hadronic medium, the degrees of freedom modify their properties, e.g. the in-medium constituent quark masses:

$$m_q^* = m_q^0 - g_s <q\bar{q}>$$

$(q = u,d,s)$

$$\Downarrow$$

$$m_q^* = m_q^0 + (m_q^V - m_q^0)\frac{<q\bar{q}>}{<q\bar{q}>_V}$$

* mean-field results (1PI)

Scalar quark condensate in the hadronic medium

- The behavior of the scalar quark condensate $\langle q\bar{q}\rangle$ in the hadronic medium (baryons + mesons) can be obtained e.g. from

B. Friman et al., Eur. Phys. J. A 3, 165, 1998

non-linear $\sigma-\omega$ model:

$$\frac{\langle q\bar{q}\rangle}{\langle q\bar{q}\rangle_V} = 1 - \frac{\Sigma_\pi}{f_\pi^2 m_\pi^2}\rho_S - \sum_h \frac{\sigma_h \rho_S^h}{f_\pi^2 m_\pi^2}$$

baryonic medium — mesonic medium

where $\Sigma_\pi \approx 45$ MeV is the pion-nucleon Σ-term,
$\sigma_h = m_\pi/2$ for light mesons;
$= m_\pi/4$ - strange mesons

1) ρ_s is the scalar density of baryonic matter :

Scalar field $\sigma(x)$ mediates the scalar interaction of baryons with the surrounding medium with a g_s coupling

from non-linear $\sigma-\omega$ model: — from PHSD

$$m_\sigma^2\sigma(x) + B\sigma^2(x) + C\sigma^3(x) = g_s\rho_S = g_s d\int \frac{d^3p}{(2\pi)^3}\frac{m_N^*(x)}{\sqrt{p^2+m_N^{*2}}} f_N(x,\mathbf{p})$$

$$m_N^*(x) = m_N^V - g_s\sigma(x)$$

- $\sigma(x)$ is determined locally by solution of the nonlinear gap equation ;
- parameters g_s , m_σ , B, C are fixed to reproduce the main nuclear matter quantities, i.e. saturation density, binding energy per nucleon, compression modulus and the effective nucleon mass.

2) ρ_s^h is the scalar density of mesons of type h ➔ from PHSD

Scalar quark condensate in HIC

PHSD:
Ratio of the scalar quark condensate

$$\frac{<q\bar{q}>}{<q\bar{q}>_V}$$

compared to the vacuum as a function of *x,z (y=0)* at different time *t* for central Au+Au collisions at 30 AGeV

- **restoration of chiral symmetry:**
  $\langle q\bar{q}\rangle/\langle q\bar{q}\rangle_V \rightarrow 0$

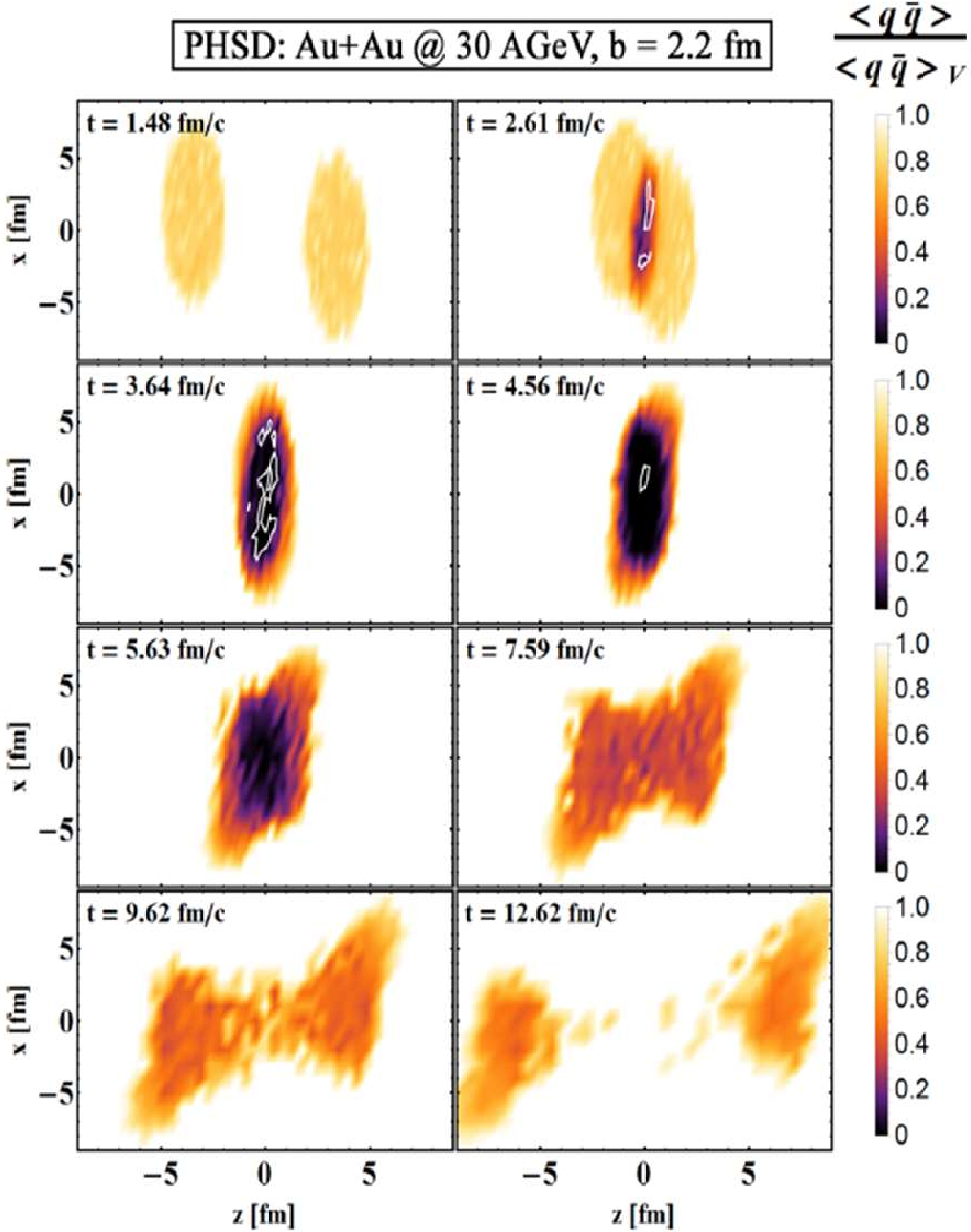

W. Cassing, A. Palmese, P. Moreau, E.L. Bratkovskaya, PRC 93, 014902 (2016), arXiv:1510.04120

Modeling of the chiral symmetry restoration in PHSD

- HIC: in the **Schwinger formula** the **in-medium constituent masses** $m^*_{q;s}$ (instead of vacuum $m_{q;s}$) have to be considered:

$$\frac{P(s\bar{s})}{P(u\bar{u})} = \frac{P(s\bar{s})}{P(d\bar{d})} = \gamma_S = \exp\left(-\pi \frac{m_S^{*2} - m_q^{*2}}{2\kappa}\right)$$

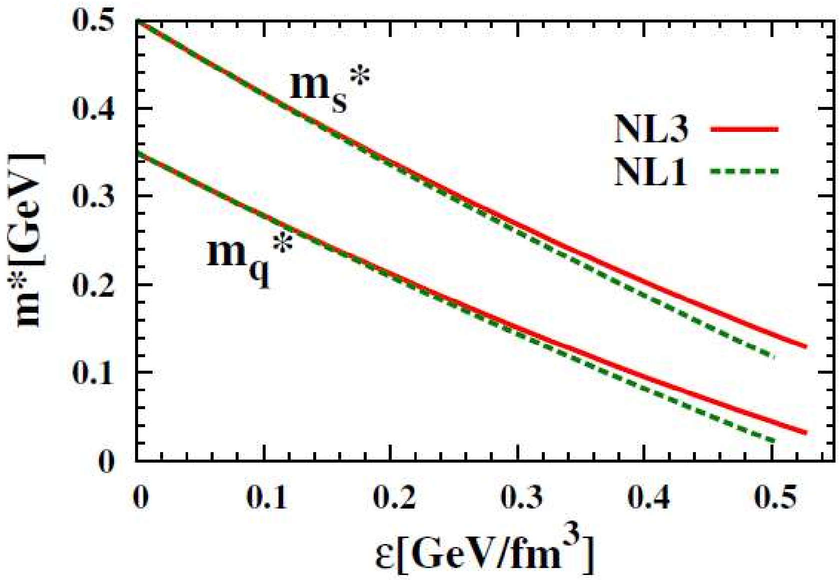

➔ **Strangeness ratio *s/u***

I. hadronic phase : $\varepsilon < \varepsilon_C$

As a consequence of the **chiral symmetry restoration (CSR)**, the **strangeness production** probability **increases** with the local energy density ε.

II. QGP: $\varepsilon > \varepsilon_C$

- In the QGP phase, for the s,u production by partonic interactions in QGP: rato s/u → 0.3

I. The ratio *s/u* in the string decay

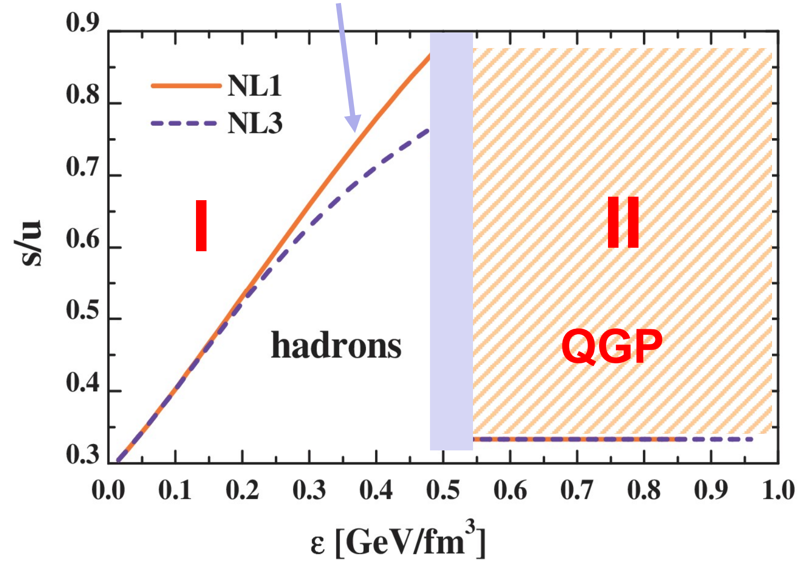

Sketch: Chiral symmetry restoration vs. deconfinement

I. Initial stage of HIC collisions:

Hadronic matter ➔ string formation

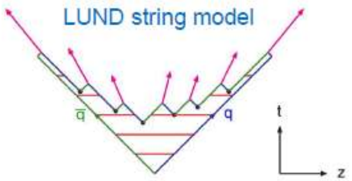

$$\frac{P(s\bar{s})}{P(u\bar{u})} = \frac{P(s\bar{s})}{P(d\bar{d})} = \gamma_S = \exp\left(-\pi \frac{m_S^{*2} - m_q^{*2}}{2\kappa}\right)$$

$$\mathbf{m}_q^* = \mathbf{m}_q^0 + (m_q^V - m_q^0)\frac{<\mathbf{q}\bar{\mathbf{q}}>}{<\mathbf{q}\bar{\mathbf{q}}>_V}$$

II. QGP

(time-like partons, explicit partonic interactions)

III. Hadronic phase

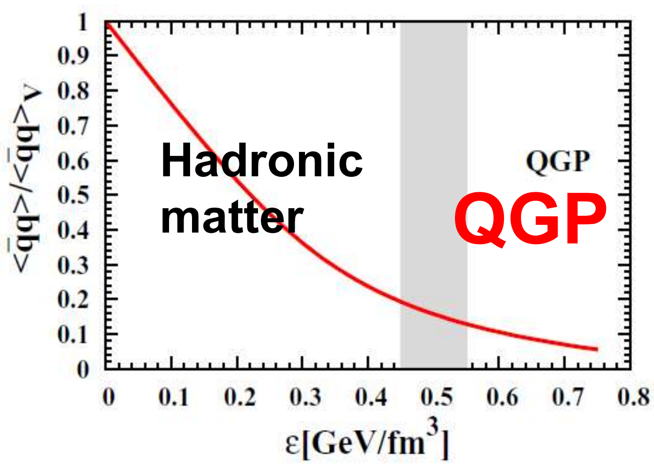

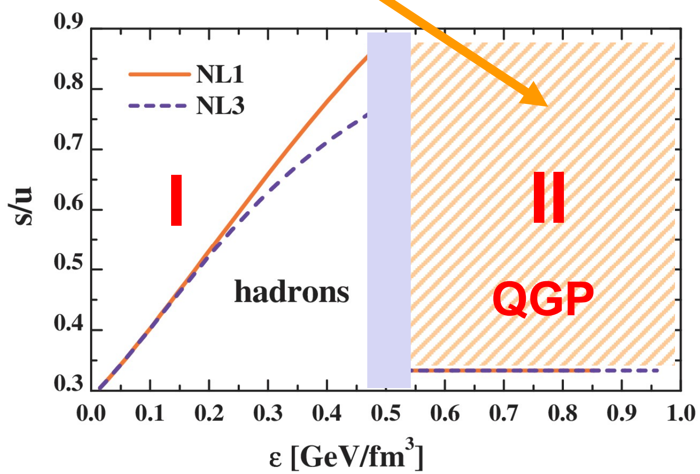

- **Chiral symmetry restoration via Schwinger mechanism (and non-linear $\sigma - \omega$ model) changes the „flavour chemistry" in string fragmentation (1PI):**
  $\langle q\bar{q}\rangle/\langle q\bar{q}\rangle_V \rightarrow 0$ ➔ $m_s^* \rightarrow m_s^0$ ➔ **s/u grows**

➔ the strangeness production probability increases with the local energy density ε (up to ε_C) due to the partial chiral symmetry restoration!

Time evolution of strangeness

The strange quark number N_s (the same for N_{sbar}) as a function of time in 5% central Au+Au collision at 30 AGeV

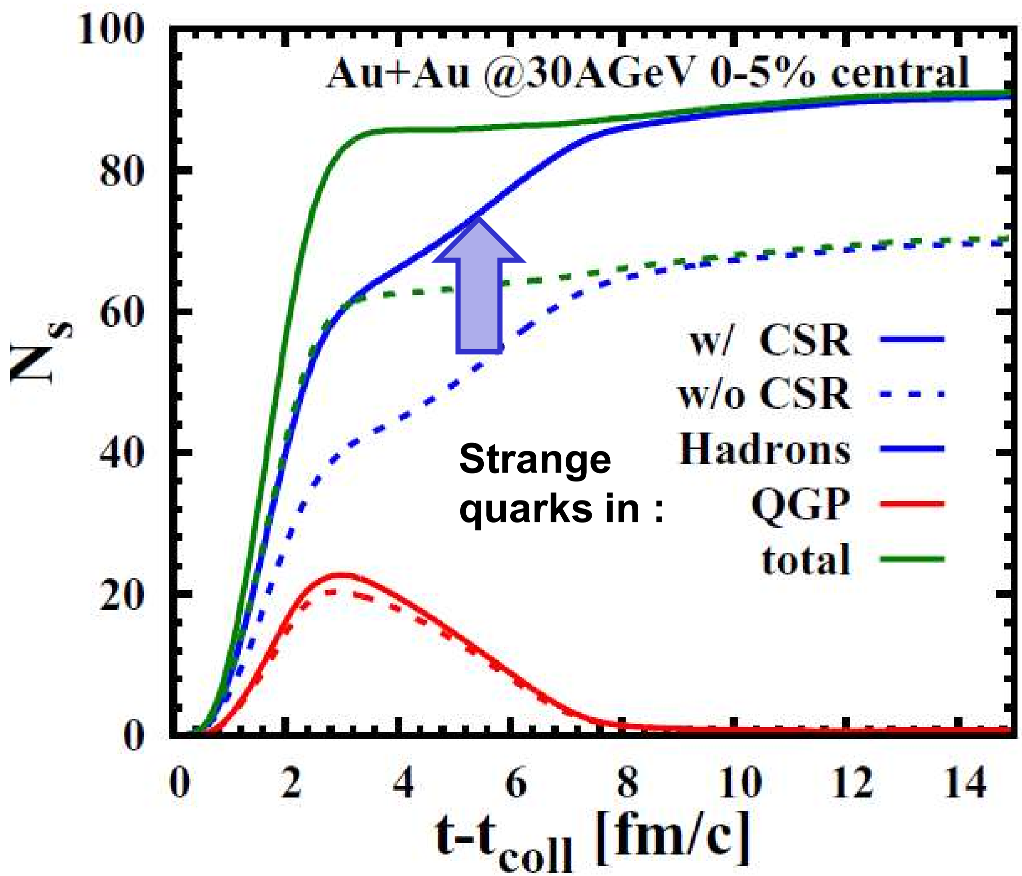

Chiral symmetry restoration leads to the enhancement of strangeness production during the string fragmentation in the beginning of HIC in the hadronic phase

PHSD results with chiral symmetry restoration (CSR)

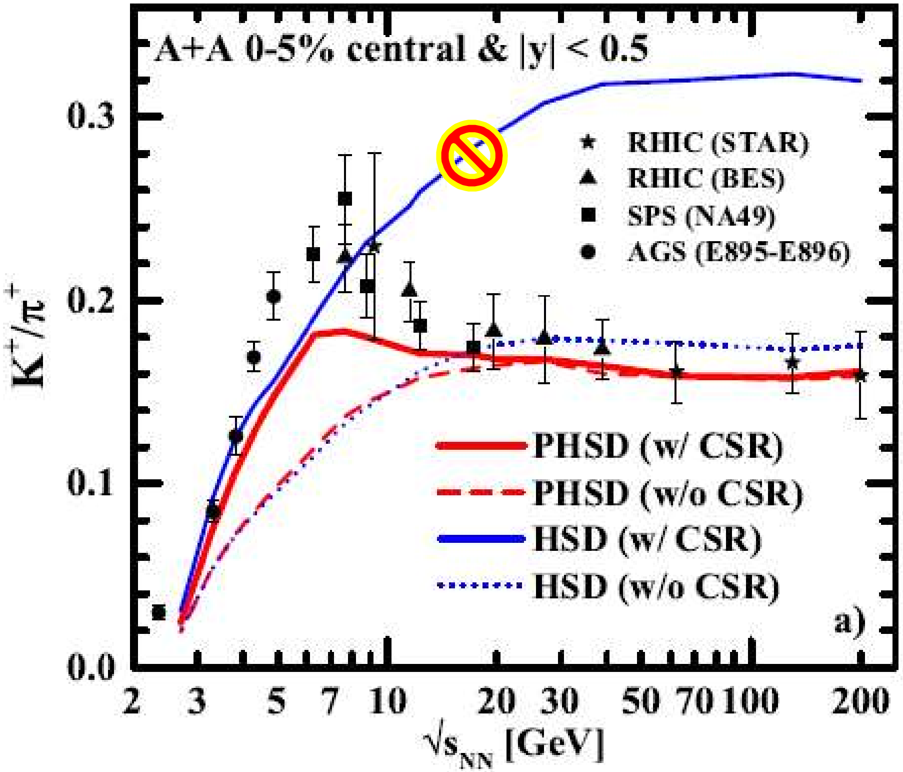

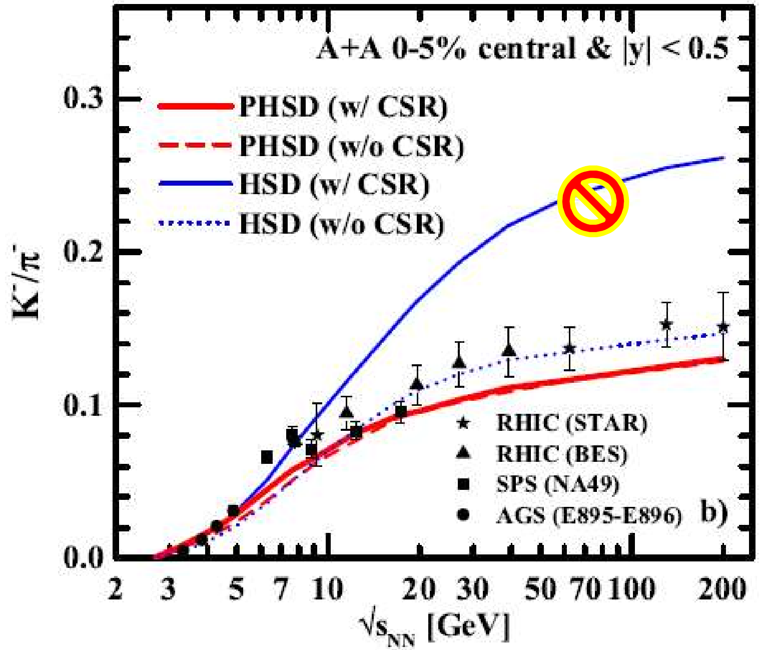

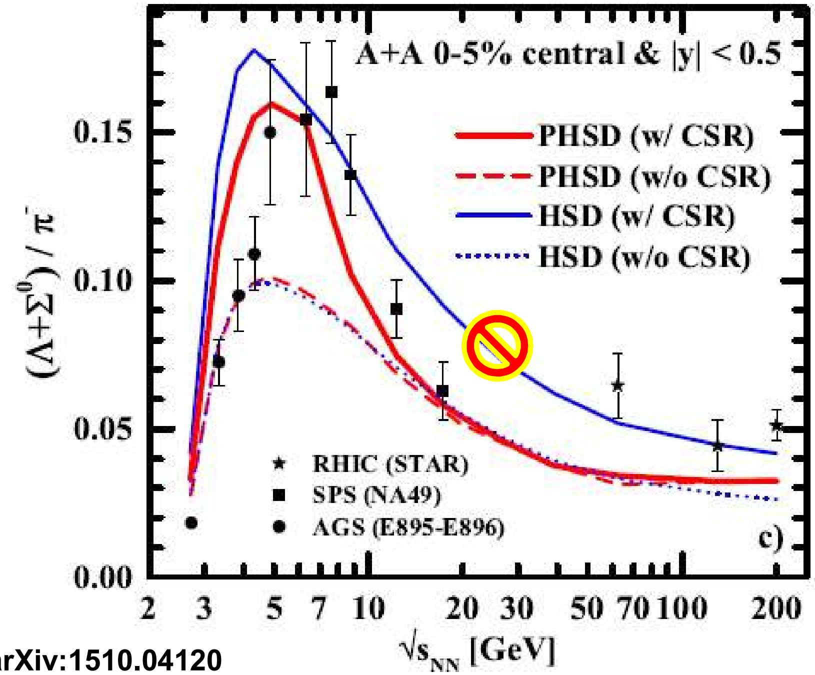

HSD with CSR: ratio K^+/π^+ grows with energy – excluded by data!

➔ **PHSD with CSR:** Maximum of K^+/π^+ ratio occurs due to the interplay between restoration of chiral symmetry in the hadronic phase and deconfinement to QGP!

W. Cassing, A. Palmese, P. Moreau, E.L. Bratkovskaya, PRC 93, 014902 (2016), arXiv:1510.04120

Excitation function of hadron ratios and yields

A. Palmese et al., PRC94 (2016) 044912 , arXiv:1607.04073

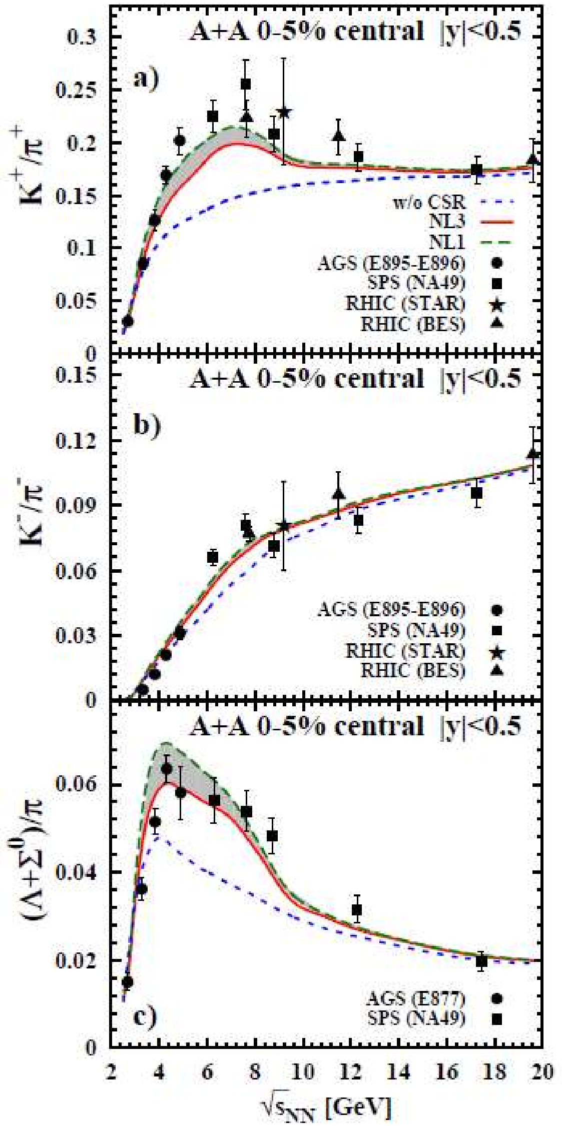

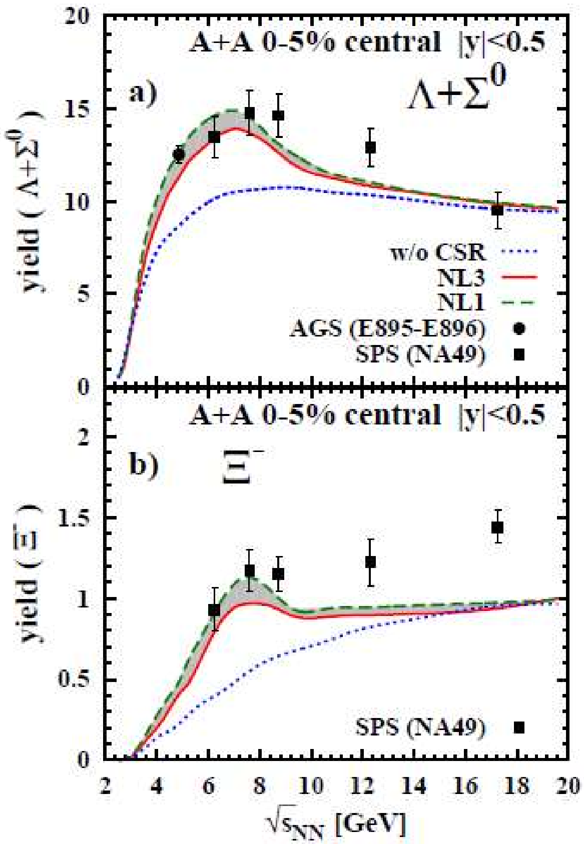

- Influence of EoS: NL1 vs NL3 ➔ low sensitivity to the nuclear EoS
- Excitation function of the hyperons $\Lambda+\Sigma^0$ and Ξ^- show analogous peaks as K^+/π^+, $(\Lambda+\Sigma^0)/\pi$ ratios due to CSR

Chiral symmetry restoration leads to the enhancement of strangeness production in string fragmentation in the beginning of HIC in the hadronic phase

Sensitivity to the system size: p+A collisions

- In p+A collisions strange to non-strange particle ratios show no peaks

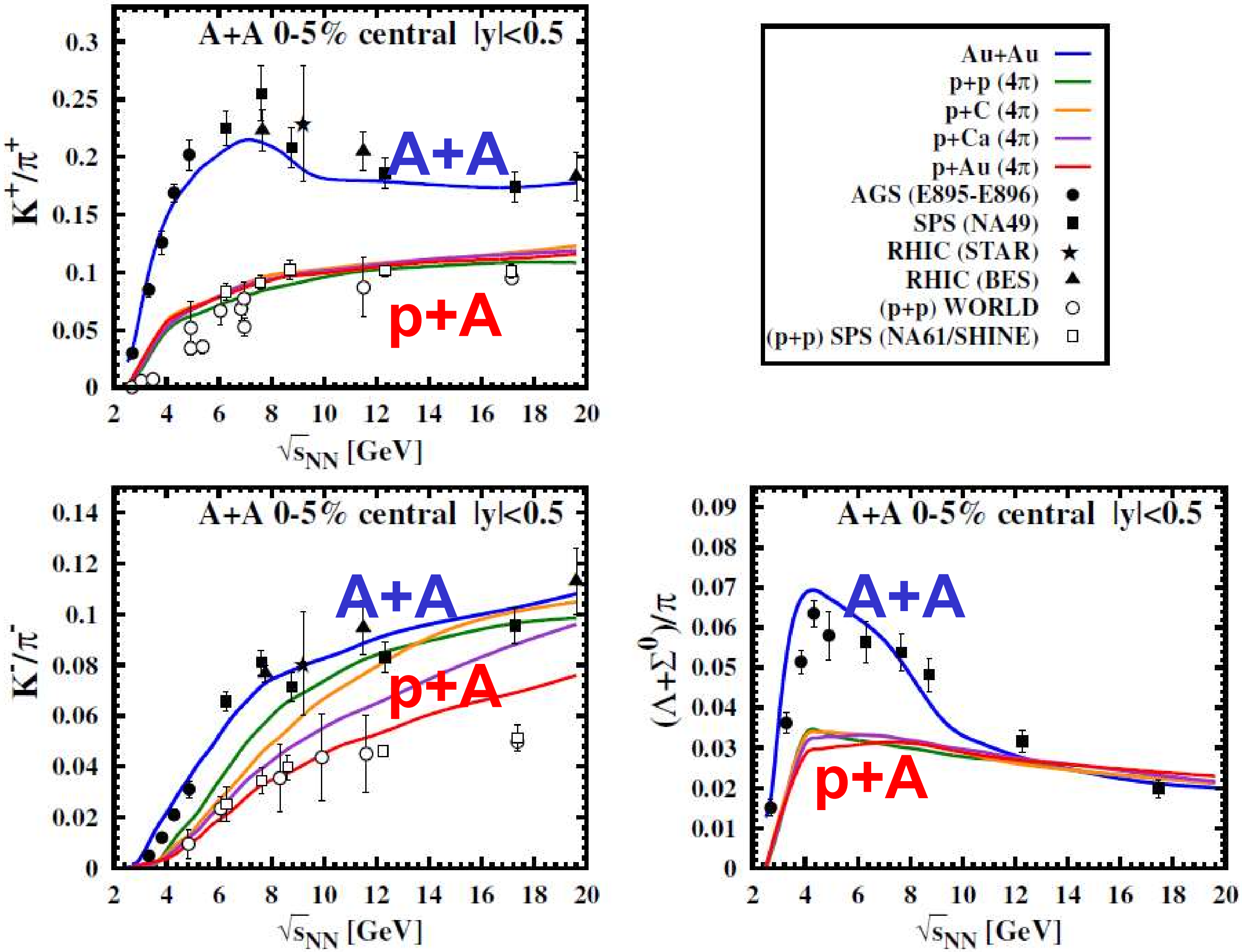

A. Palmese et al., PRC94 (2016) 044912 , arXiv:1607.04073

PHSD vs. statistical model

THERMUS: J. Cleymans et al., arXiv:1603.09553

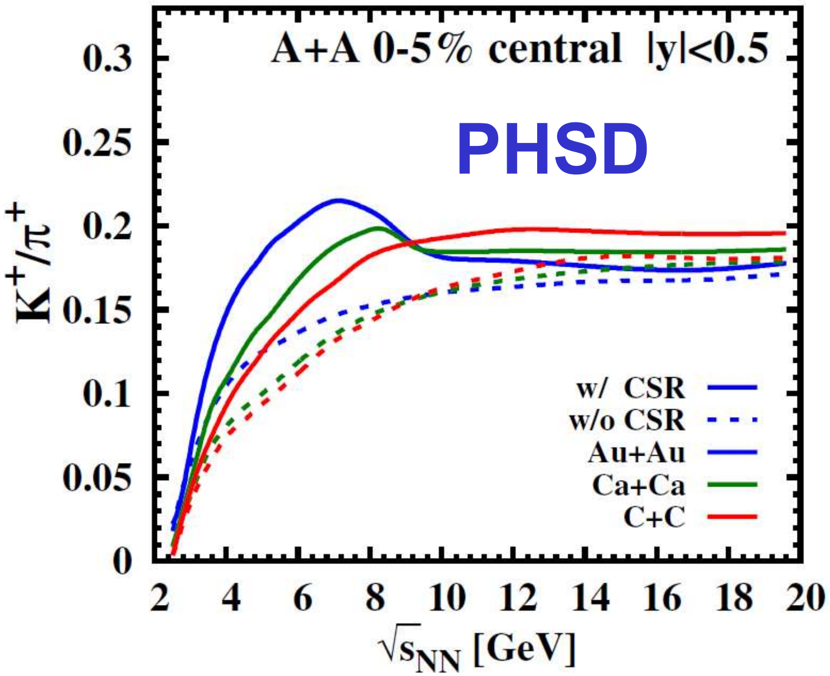

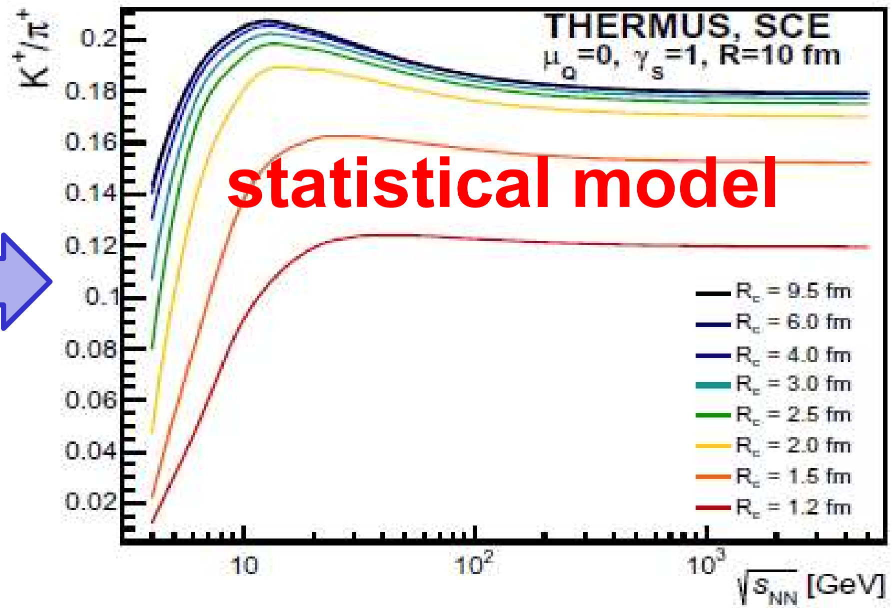

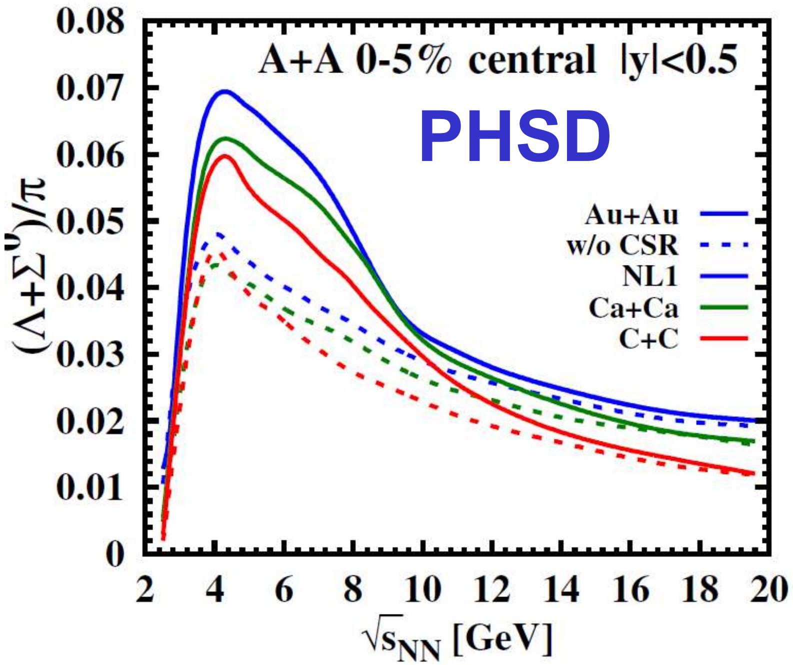

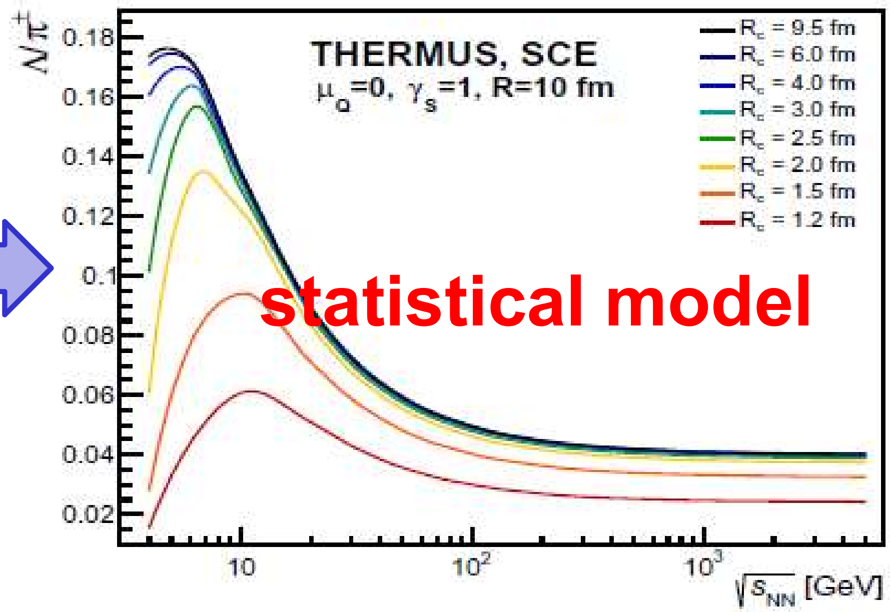

m_T spectra of pions and $K^{+/-}$ at AGS energies

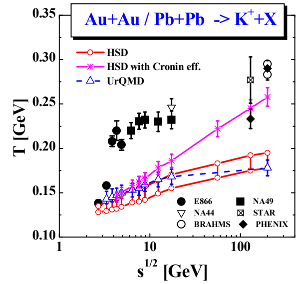

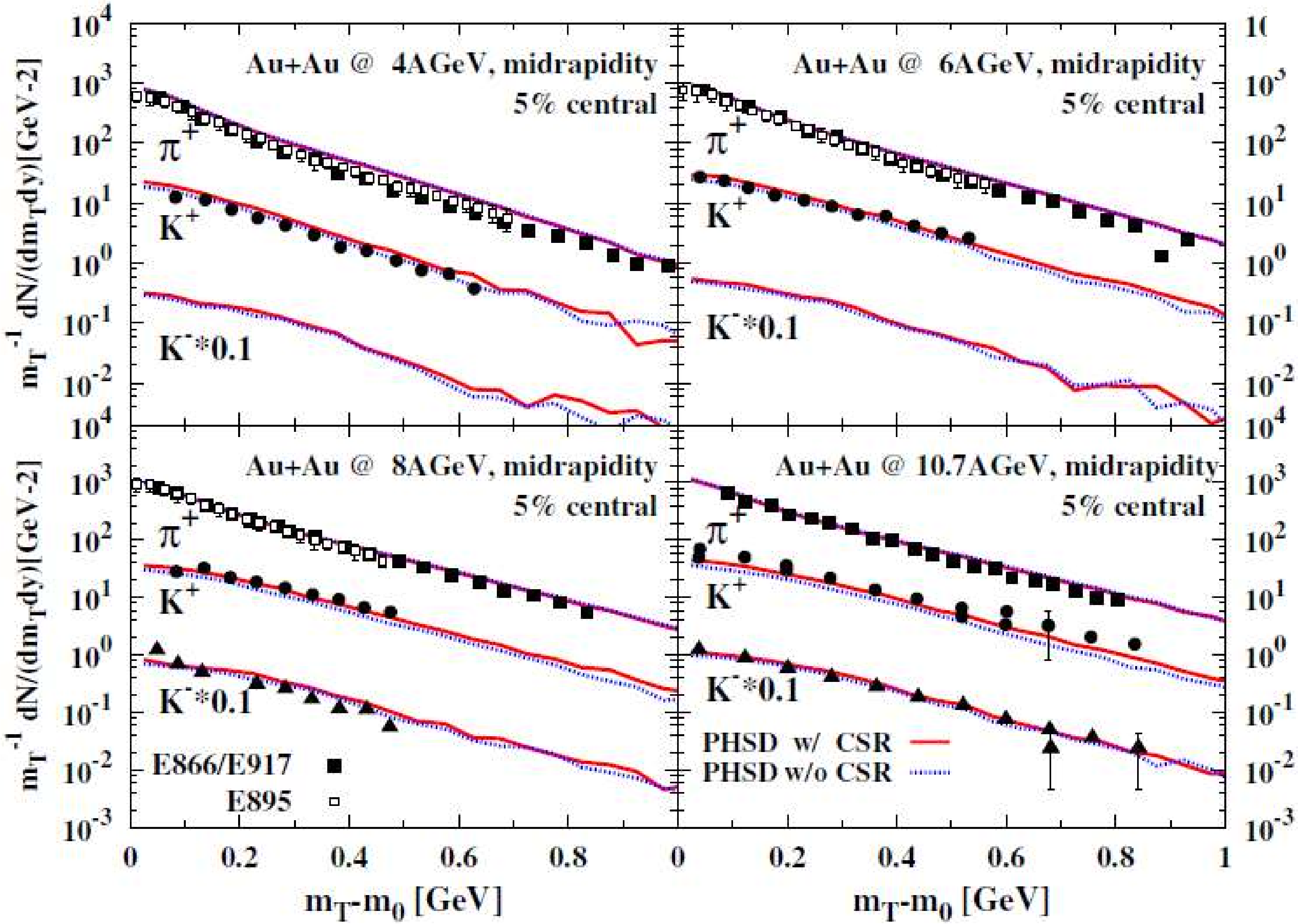

A. Palmese et al., PRC94 (2016) 044912 , arXiv:1607.04073

m_T spectra of pions and $K^{+/-}$ at SPS energies

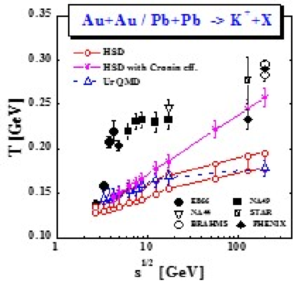

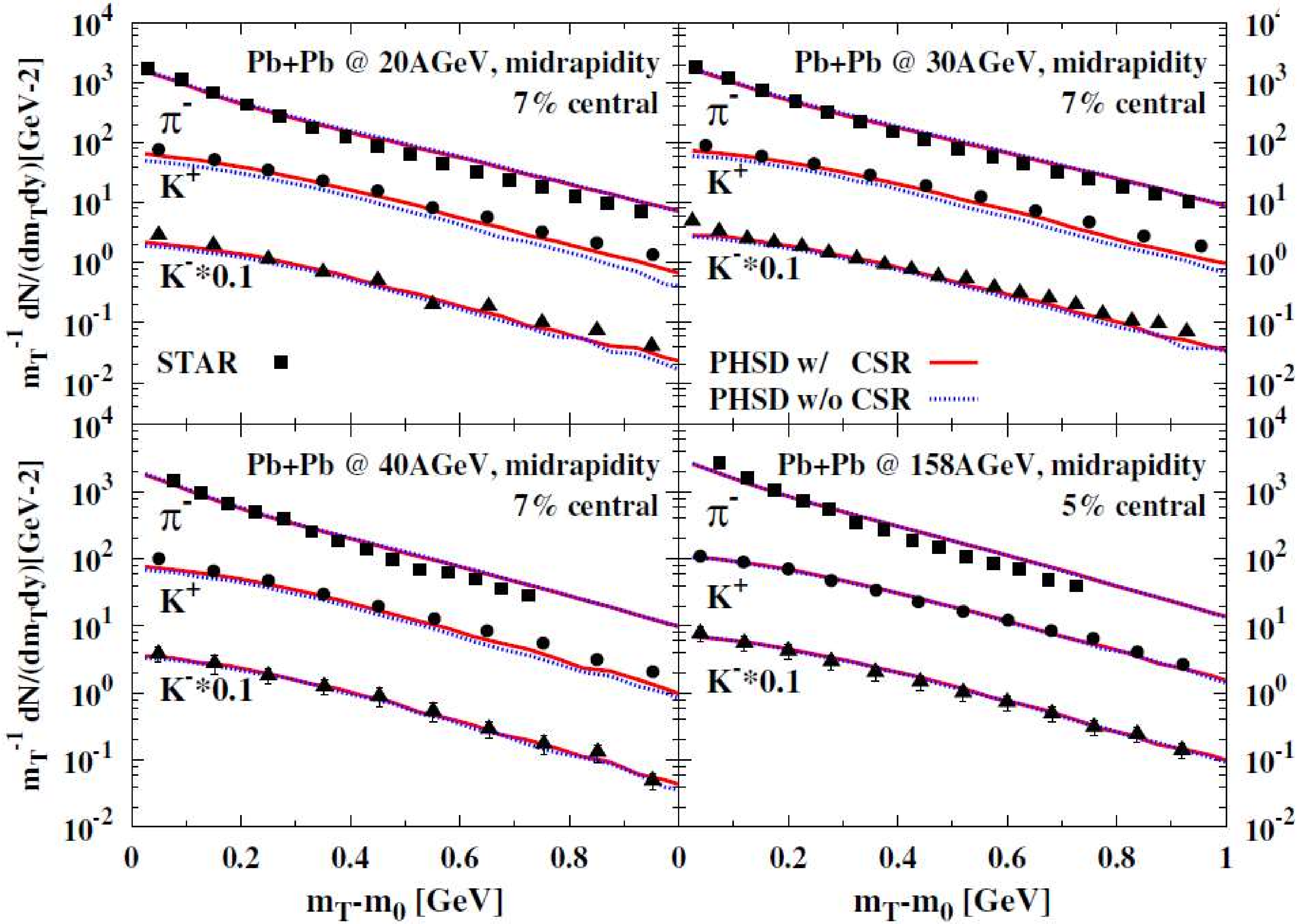

A. Palmese et al., PRC94 (2016) 044912 , arXiv:1607.04073

Excitation function of T_{eff}

Alessia Palmese

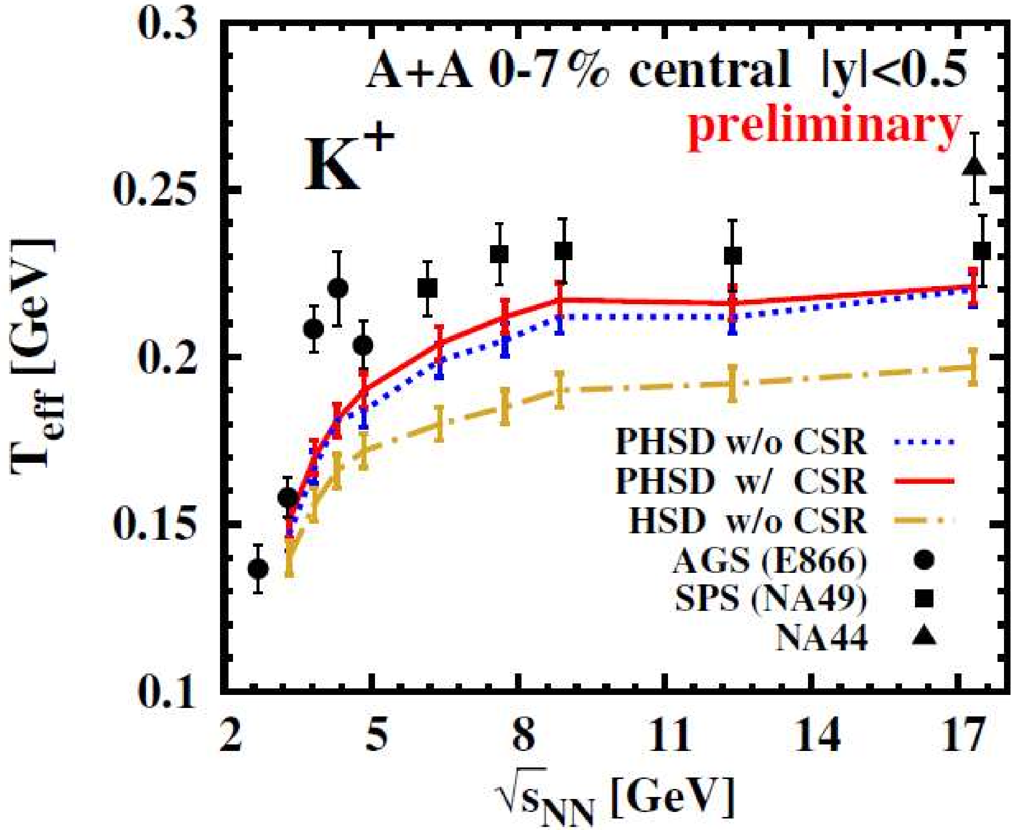

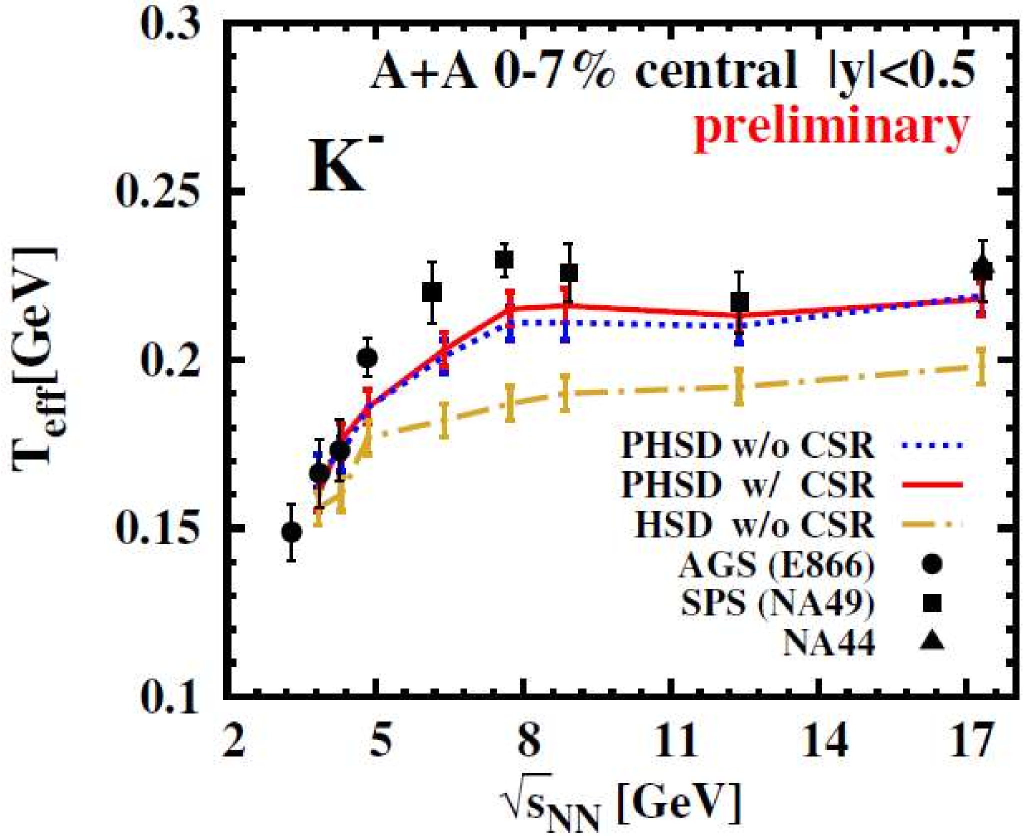

→ **Increase of slope T_{eff} due to the QGP**

→ **Small effect of chiral symmetry restoration on slope Teff**

Thermodynamics of strangeness in HIC

- Which parts of the phase diagram in the (T, μ_B)-plane are probed by heavy-ion collisions via the strangeness production?

Non-equilibrium
(dominant strangeness production at the early stage)

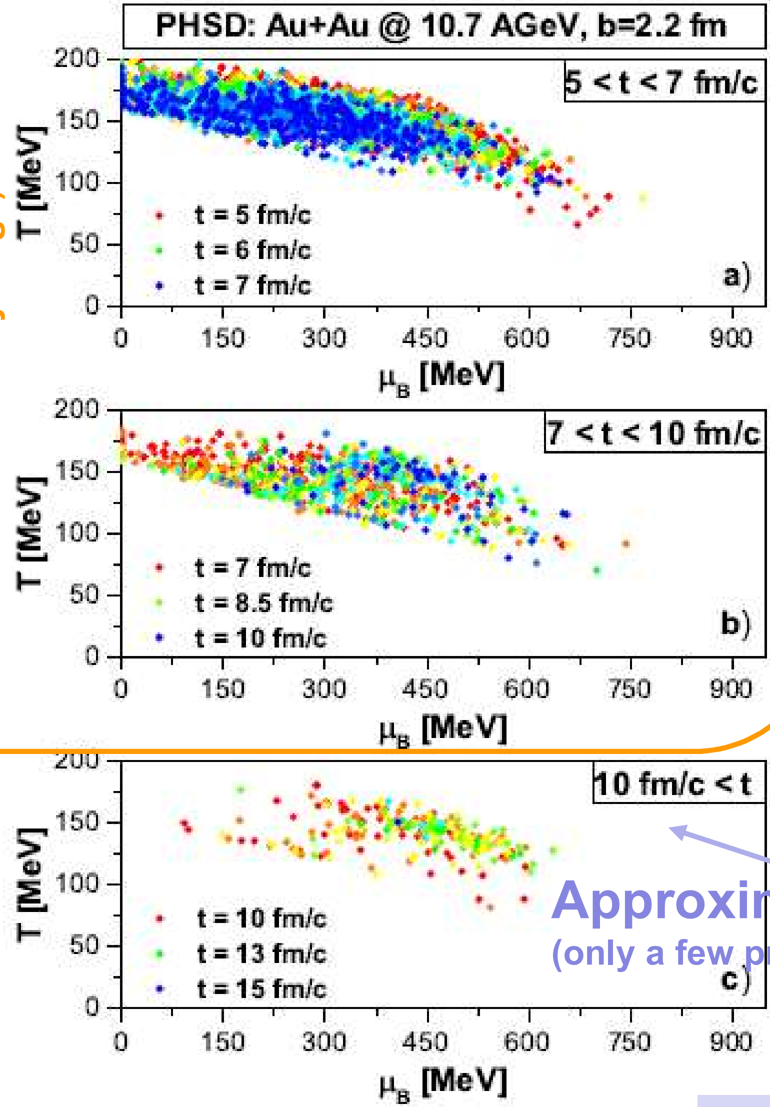

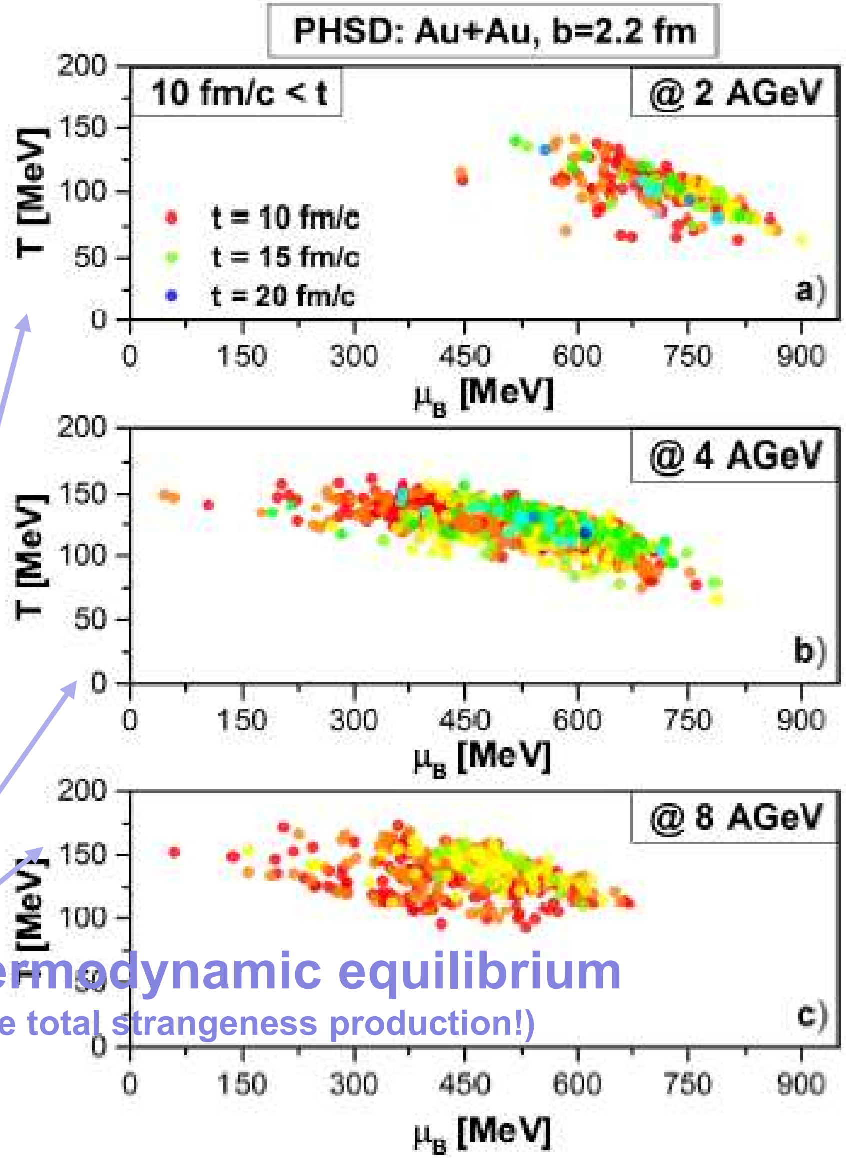

Approximate thermodynamic equilibrium
(only a few present of the total strangeness production!)

→ the spread in T and μ_B is very large !

* T here corresponds to the pion, nucleon gas, i.e. a real T is smaller!

A. Palmese et al., PRC94 (2016) 044912 , arXiv:1607.04073

Summary: CSR / QGP

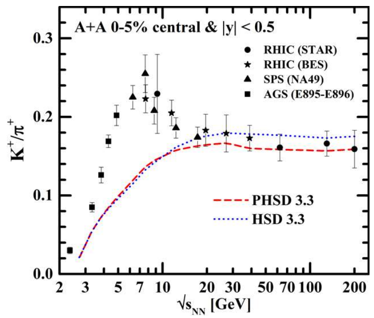

CSR / QGP

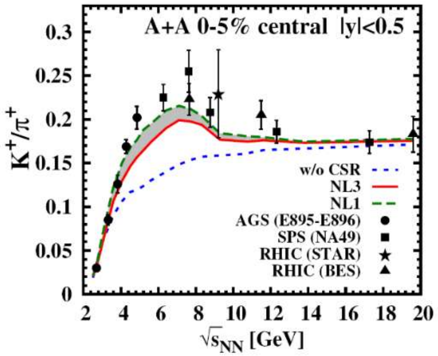

- The strangeness 'enhancement' ('horn') seen experimentally by NA49 and STAR at a bombarding energies ~20-30 A GeV (FAIR/NICA energies!) cannot be attributed only to deconfinement
- Including essential aspects of chiral symmetry restoration in the hadronic phase, we observe a rise in the K^+/π^+ ratio at low $\sqrt{s_{NN}}$ and then a drop due to the appearance of a deconfined partonic medium → a 'horn' emerges

→ The 'horn' in the K^+/π^+ ratio is due to an interplay between CRS and deconfinement

- Hardening of m_T spectra due to the QGP

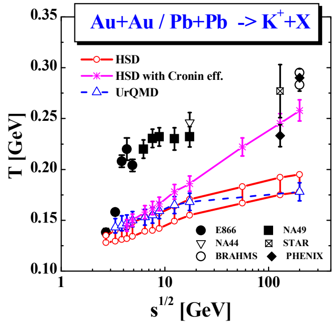

QGP

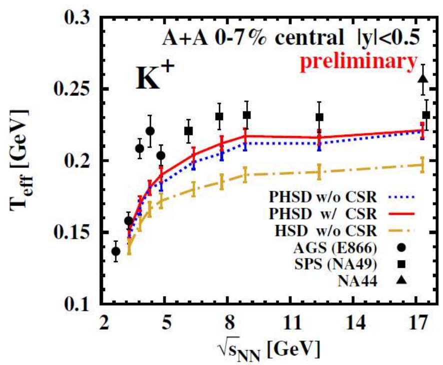

Collective flow, anisotropy coefficients (v_1, v_2, ...) in A+A

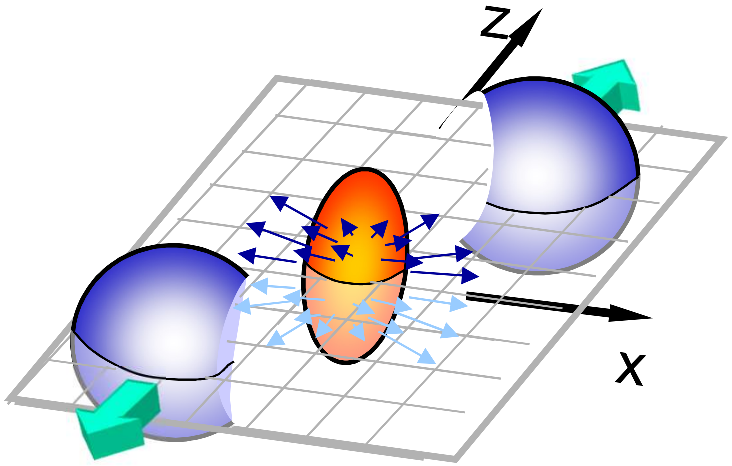

Anisotropy coefficients v_n

Non central Au+Au collisions :

- interaction between constituents leads to a **pressure gradient**
→ **spatial asymmetry** is converted to an **asymmetry in momentum space** → **collective flow**

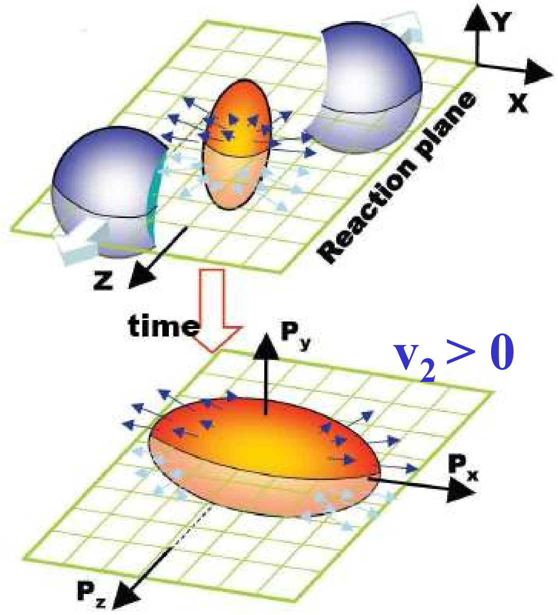

$$\frac{dN}{d\varphi} \propto \left(1 + 2\sum_{n=1}^{+\infty} v_n \cos\left[n(\varphi - \psi_n)\right]\right)$$

$$v_n = \left\langle \cos n\left(\varphi - \psi_n\right)\right\rangle, \quad n = 1,2,3..,$$

$$v_1 = \left\langle \frac{p_x}{p_T} \right\rangle, \quad v_2 = \left\langle \frac{p_x^2 - p_y^2}{p_x^2 + p_y^2} \right\rangle$$

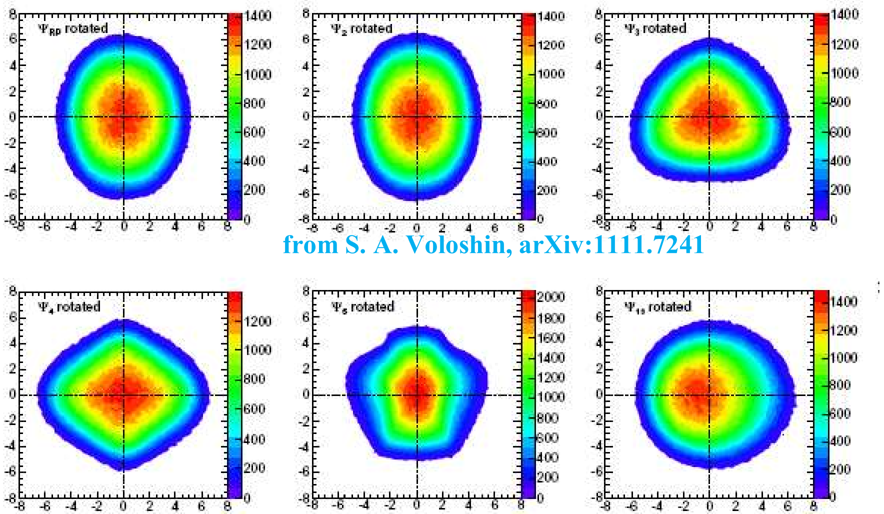

from S. A. Voloshin, arXiv:1111.7241

v_1: directed flow
v_2: elliptic flow
v_3: triangular flow

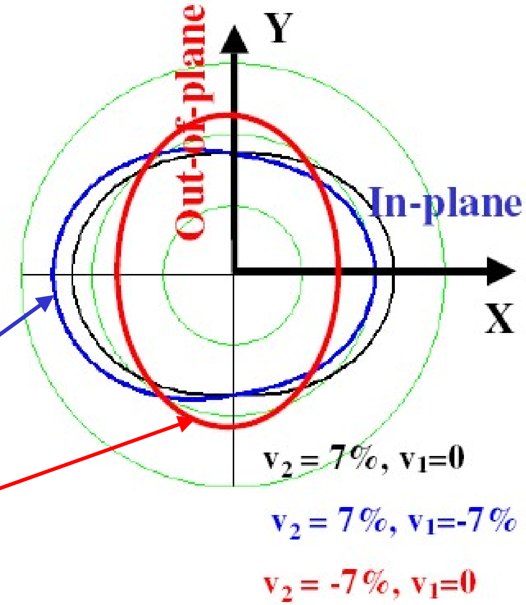

$v_2 > 0$ indicates in-plane emission of particles
$v_2 < 0$ corresponds to a squeeze-out perpendicular to the reaction plane (out-of-plane emission)

Collective flow: v_2 excitation functions

The excitation function for v_2 of charged particles from string-hadron transport models :

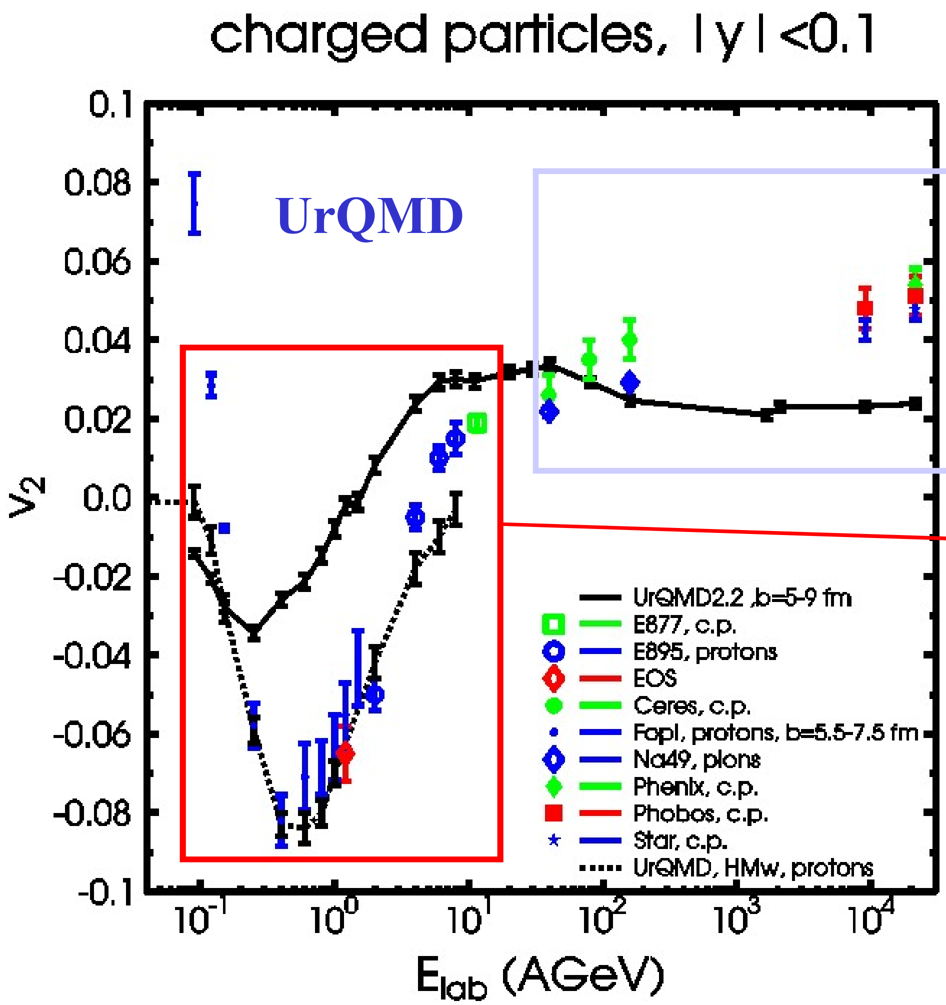

QGP

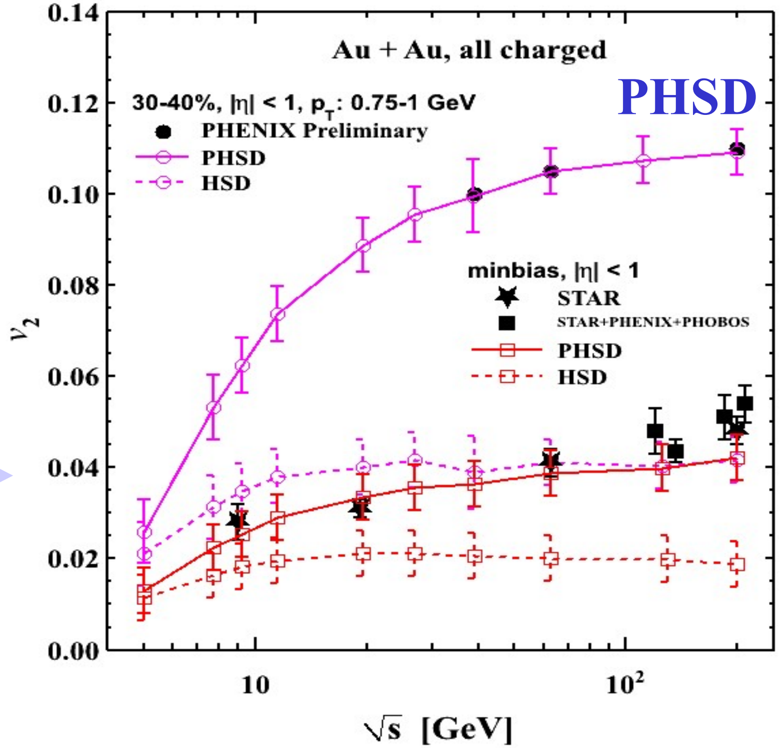

Influence of hadron potentials ➔ EoS

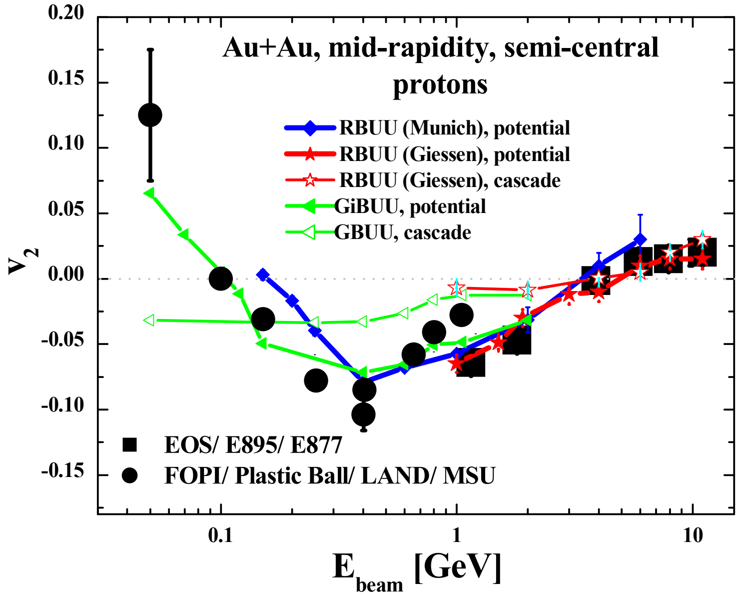

Transport model PHSD: elliptic flow v_2

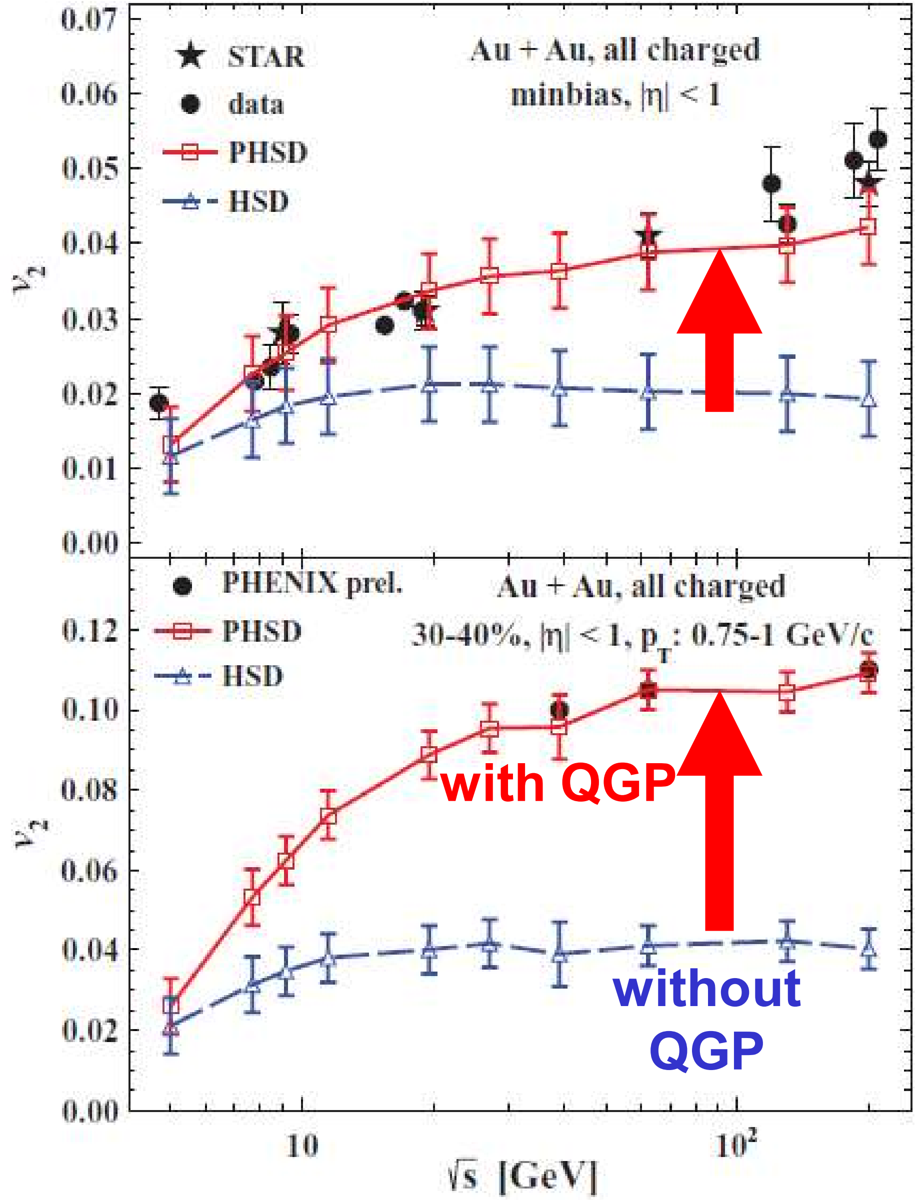

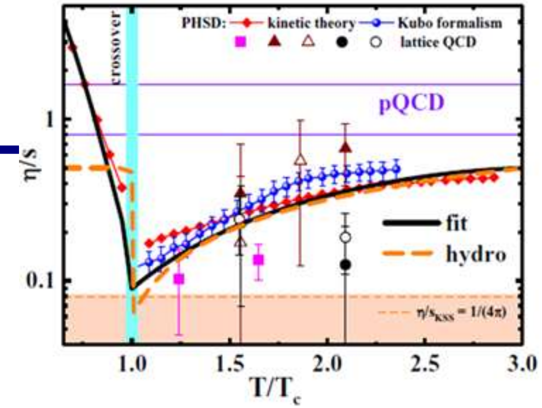

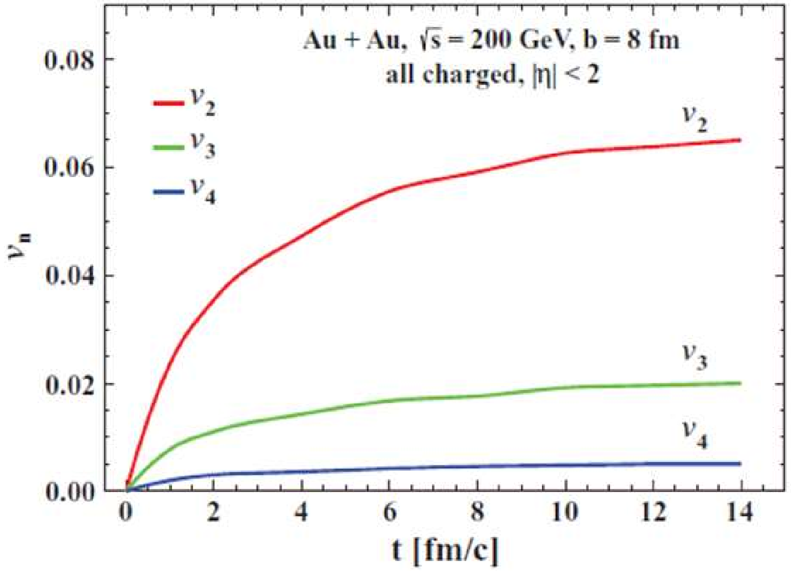

- v_2 in PHSD is larger than in HSD due to the repulsive scalar mean-field potential $U_s(\rho)$ for partons
- v_2 grows with bombarding energy due to the increase of the parton fraction

V. Konchakovski, E. Bratkovskaya, W. Cassing, V. Toneev, V. Voronyuk, Phys. Rev. C 85 (2012) 011902

V_n (n=2,3,4,5) of charged particles from PHSD at LHC

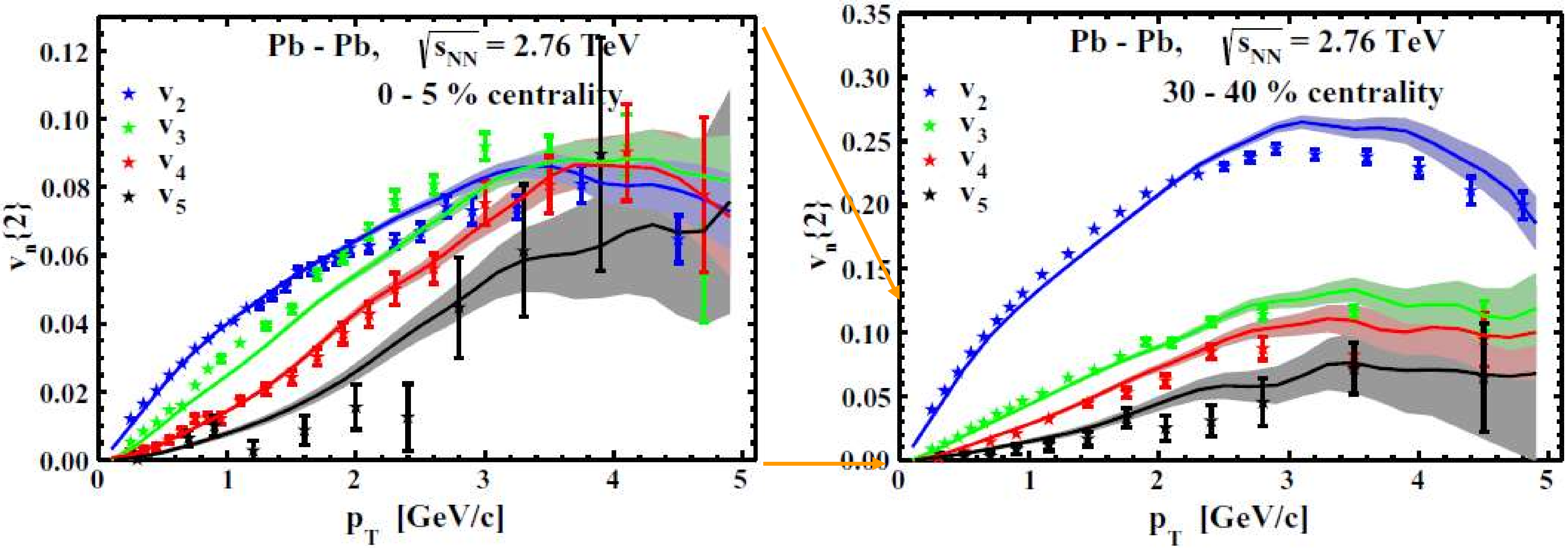

- PHSD: increase of v_n (n=2,3,4,5) with p_T
- v_2 increases with decreasing centrality
- v_n (n=3,4,5) show weak centrality dependence

symbols – ALICE

PRL 107 (2011) 032301

lines – PHSD (e-by-e)

v_n (n=3,4,5) develops by interaction in the QGP and in the final hadronic phase

V. Konchakovski, W. Cassing, V. Toneev, J. Phys. G: Nucl. Part. Phys 42 (2015) 055106

Dileptons as a probe of the QGP and in-medium effects

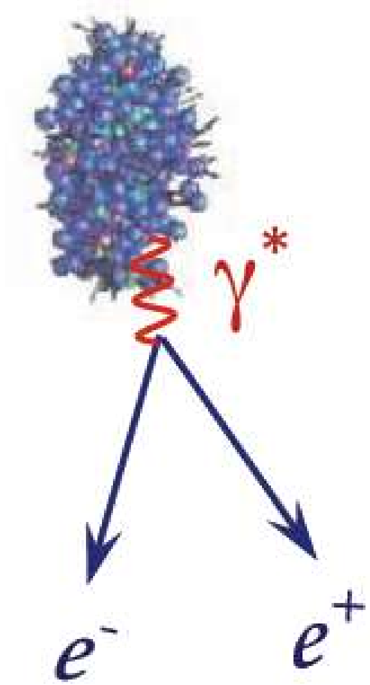

Dilepton sources

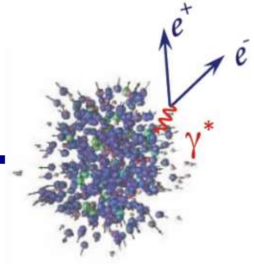

- **from the QGP via partonic (q,qbar, g) interactions:**

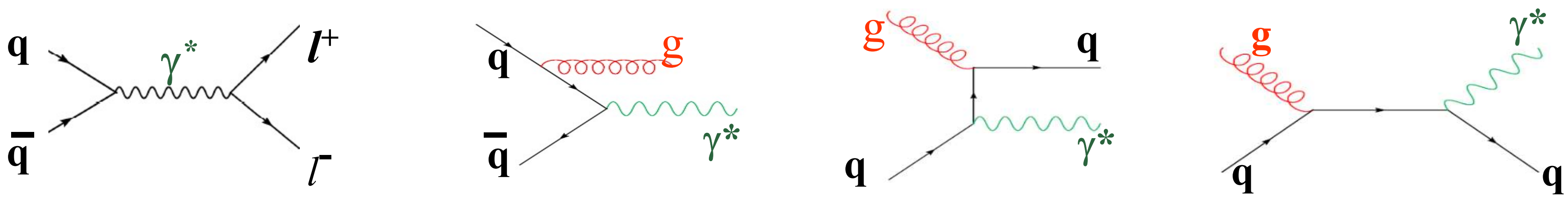

- **from hadronic sources:**

in-medium effects

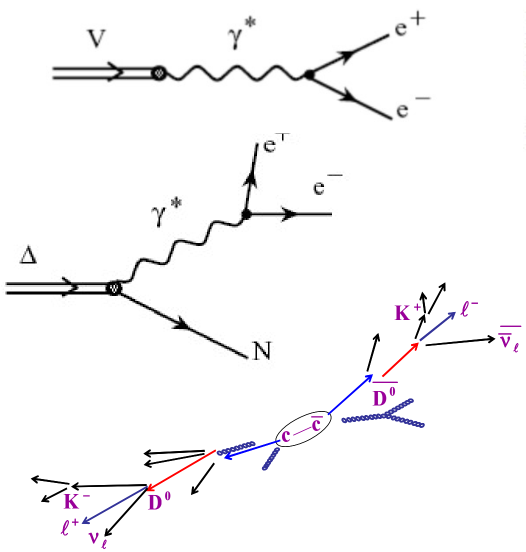

Plot from A. Drees

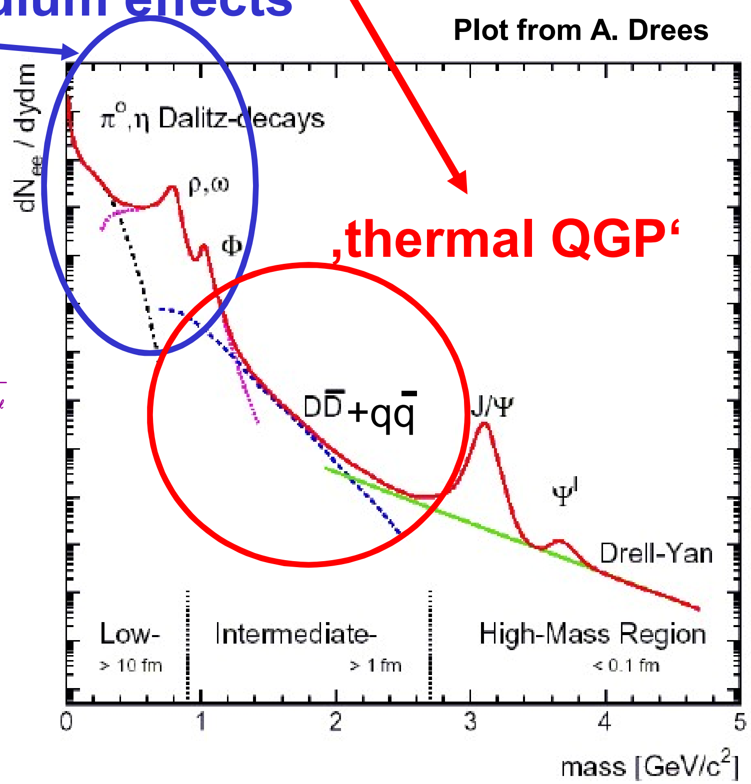

,thermal QGP'

- **direct decay of vector mesons** ($\rho,\omega,\phi,J/\Psi,\Psi'$)
- **Dalitz decay of mesons and baryons** ($\pi^0,\eta,\Delta,\ldots$)
- **correlated D+Dbar pairs**
- **radiation from multi-meson reactions** ($\pi+\pi$, $\pi+\rho$, $\pi+\omega$, $\rho+\rho$, $\pi+a_1$) - ,4π'

! Advantage of dileptons:
additional „degree of freedom" (*M*) allows to disentangle various sources

Dileptons at RHIC and LHC

RHIC

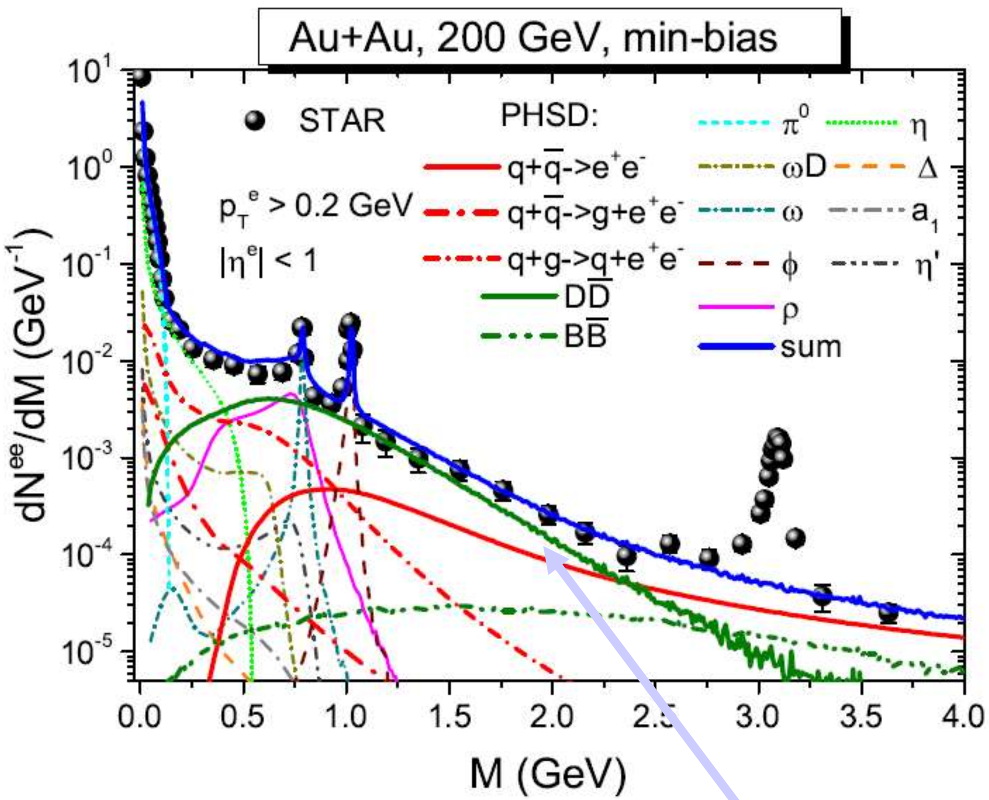

LHC

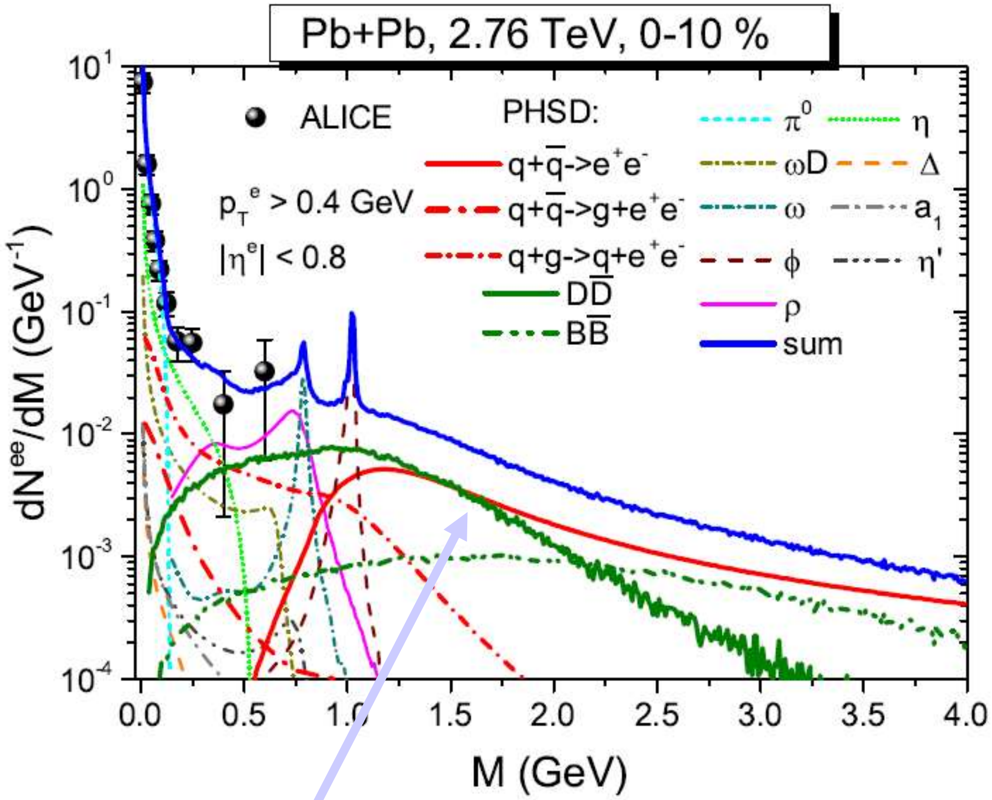

Message:

STAR data at 200 GeV and the ALICE data at 2.76 TeV are described by PHSD within

1) a collisional broadening scenario for the vector meson spectral functions
+ QGP + correlated charm

2) Charm contribution is dominant for 1.2 < M < 2.5 GeV

T. Song, W.Cassing, P.Moreau and E.Bratkovskaya, Phys. Rev. C 97 (2018) 064907

Dileptons from RHIC BES: STAR

T. Song, W.Cassing, P.Moreau and E.Bratkovskaya, Phys. Rev. C 97 (2018) 064907

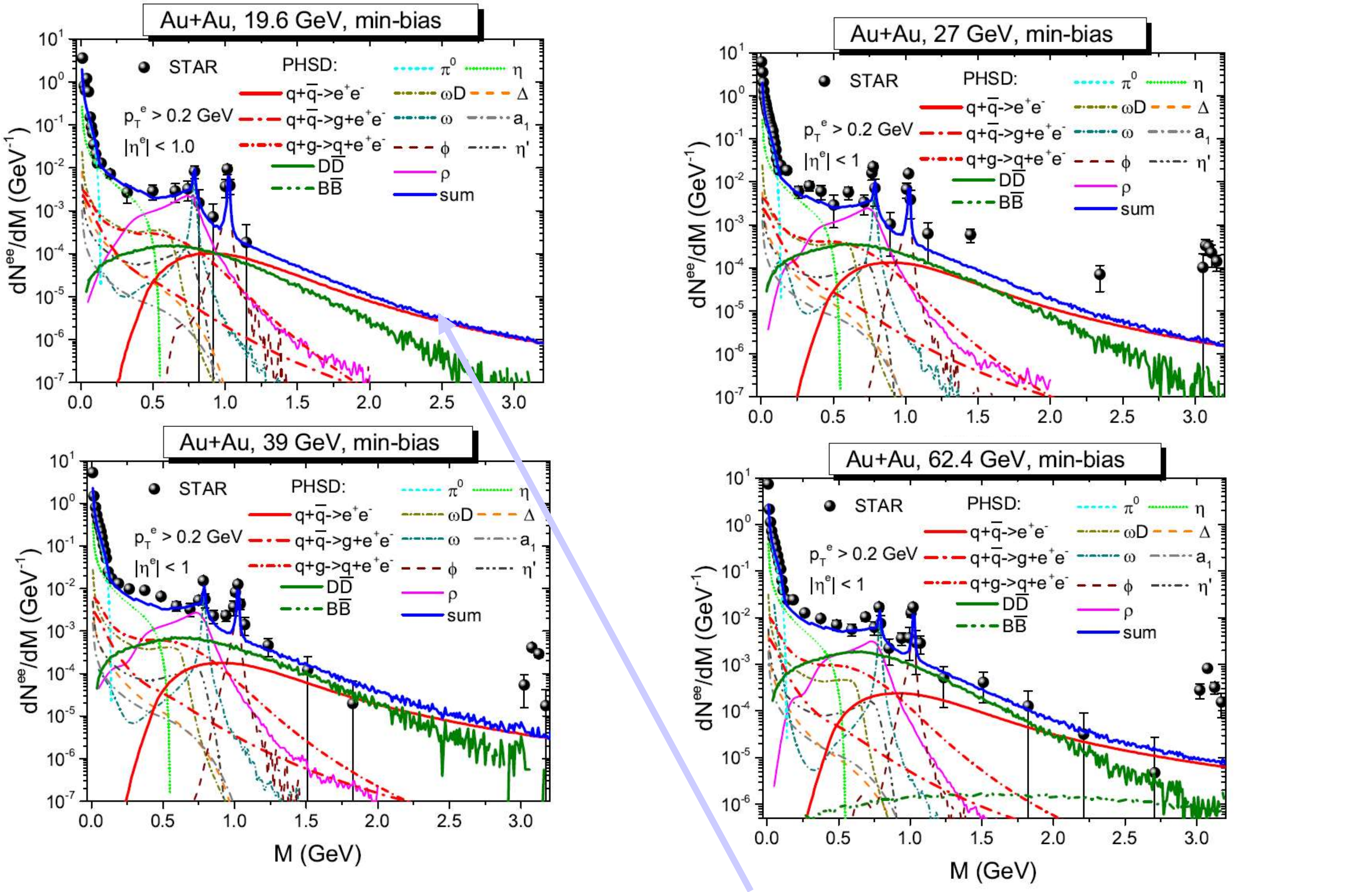

QGP and charm are dominant contributions for intermediate masses at BES RHIC
➔ measurements of charm at BES RHIC are needed to control charm production !

Dileptons at FAIR/NICA energies: predictions

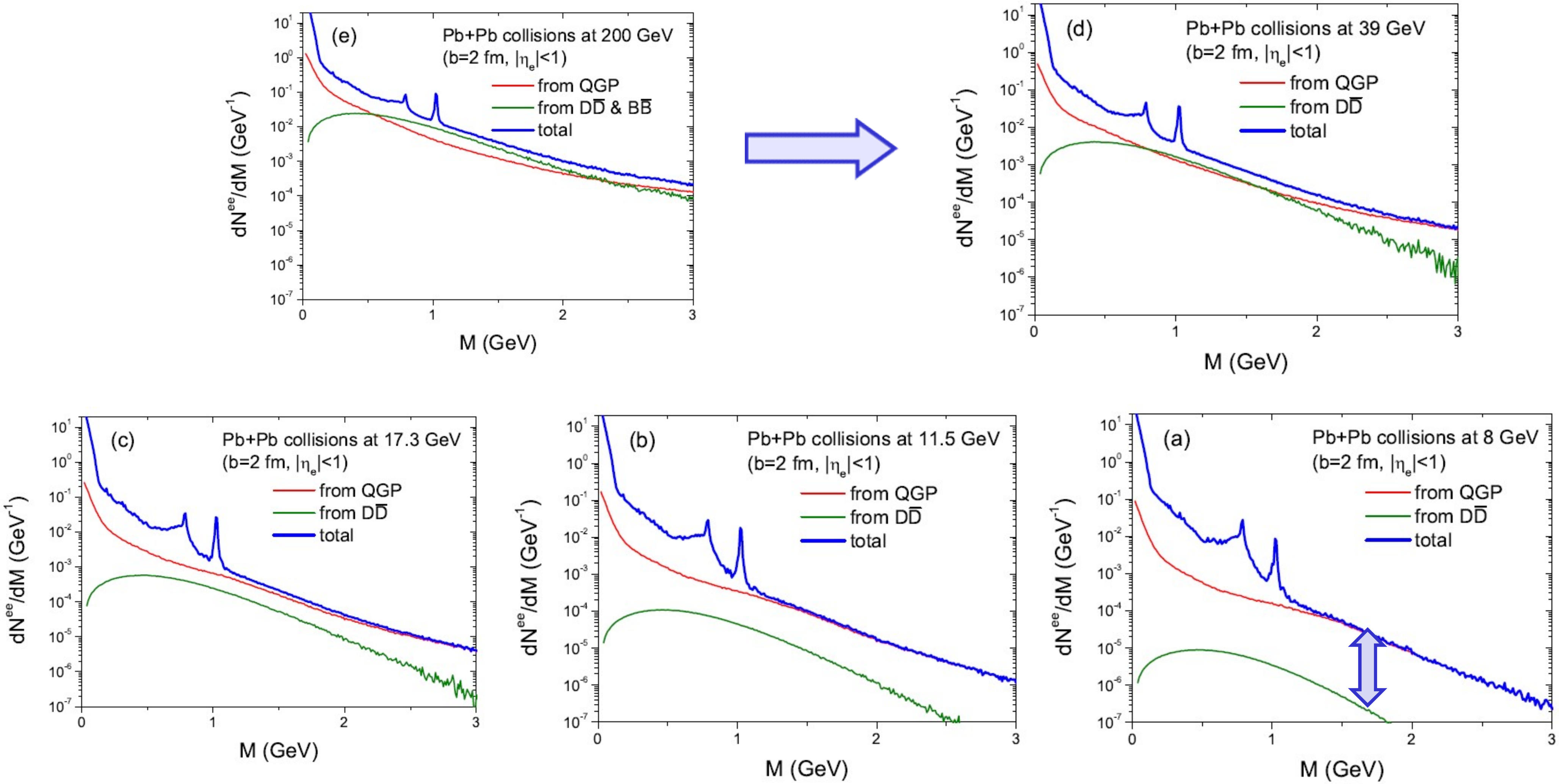

Relative contribution of QGP versus charm increases with decreasing energy!

T. Song, W.Cassing, P.Moreau and E.Bratkovskaya, Phys. Rev. C 97 (2018) 064907

Dileptons: QGP vs charm

Excitation function of dilepton multiplicity integrated for 1.2<M<3GeV

mid-rapidity

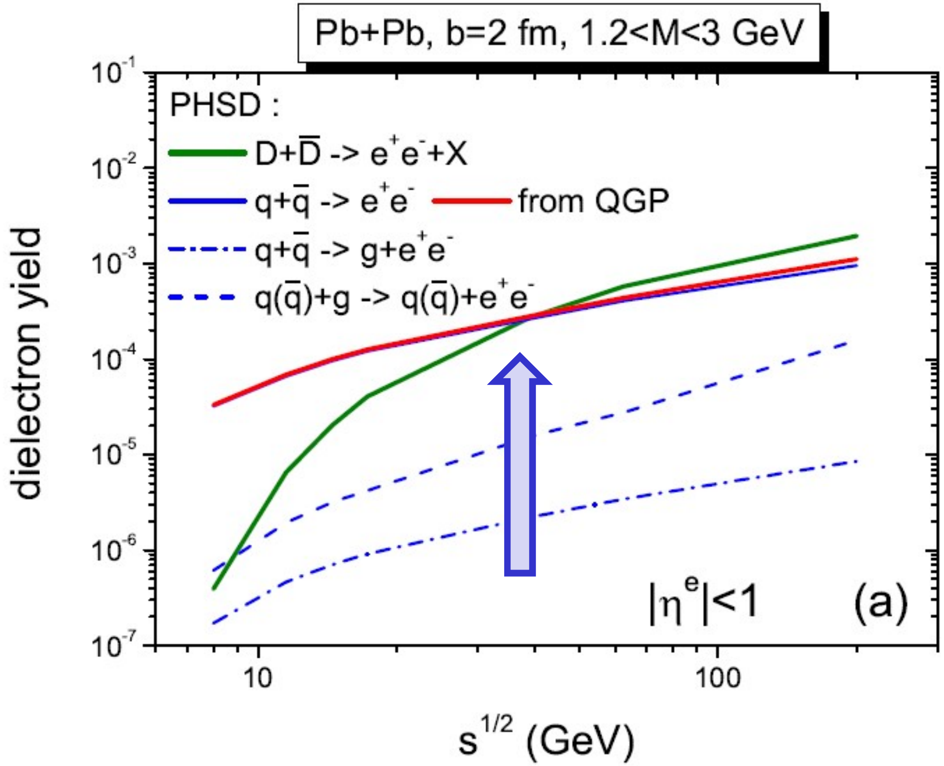

all rapidities (4π)

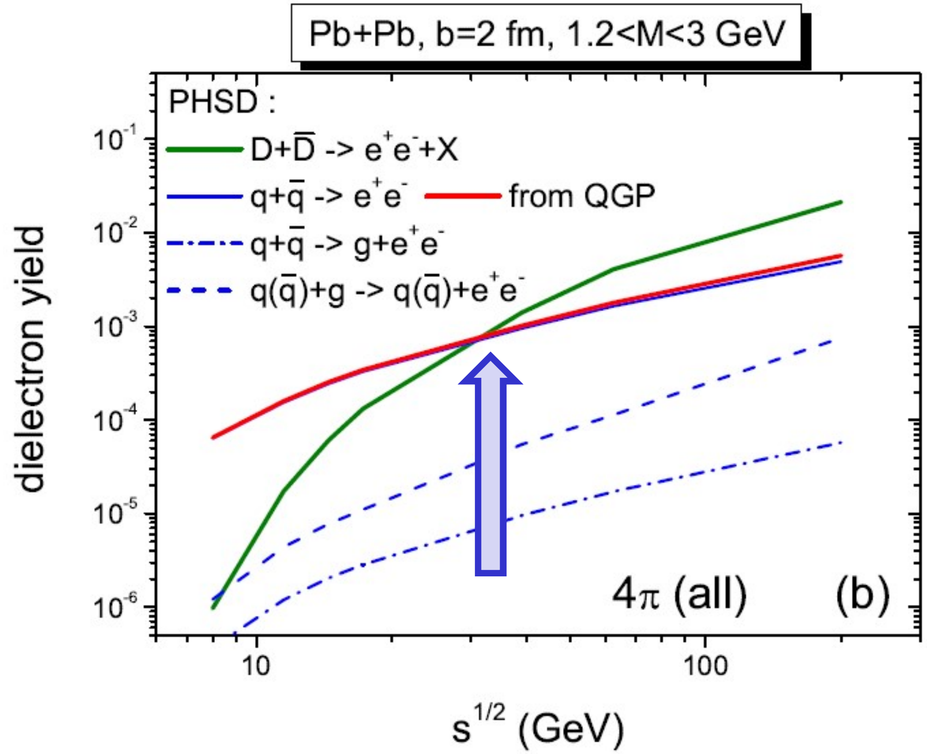

QGP contribution overshines charm with decreasing energy!
➔ Good perspectives for FAIR/NICA and BES RHIC!

T. Song, W.Cassing, P.Moreau and E.Bratkovskaya, Phys. Rev. C 97 (2018) 064907

Dilepton transverse mass spectra

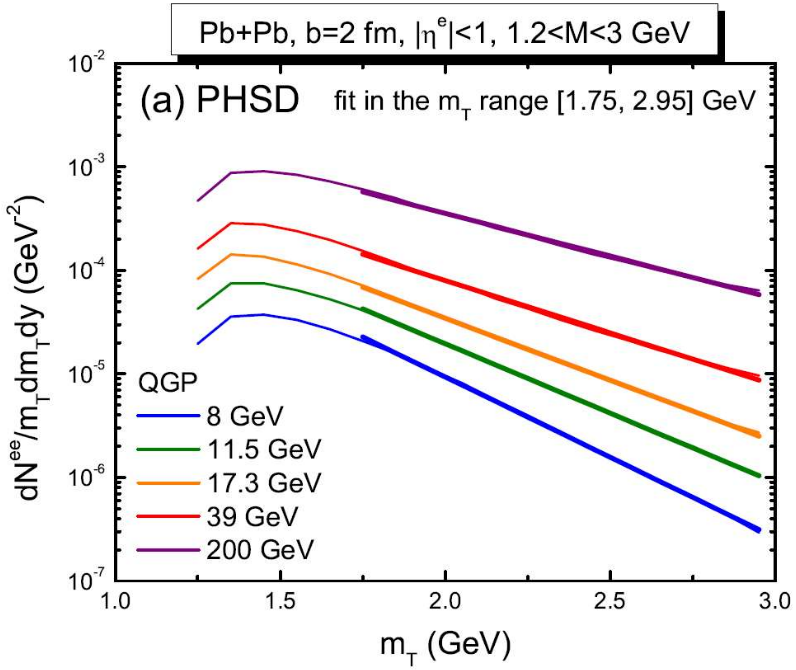

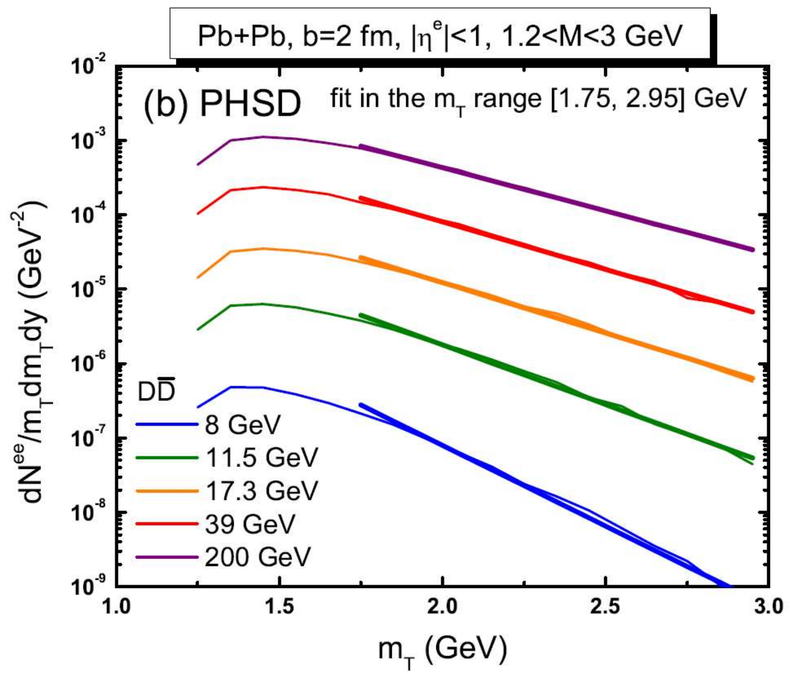

The inverse slope parameter in the mass range [1.75,2.95]

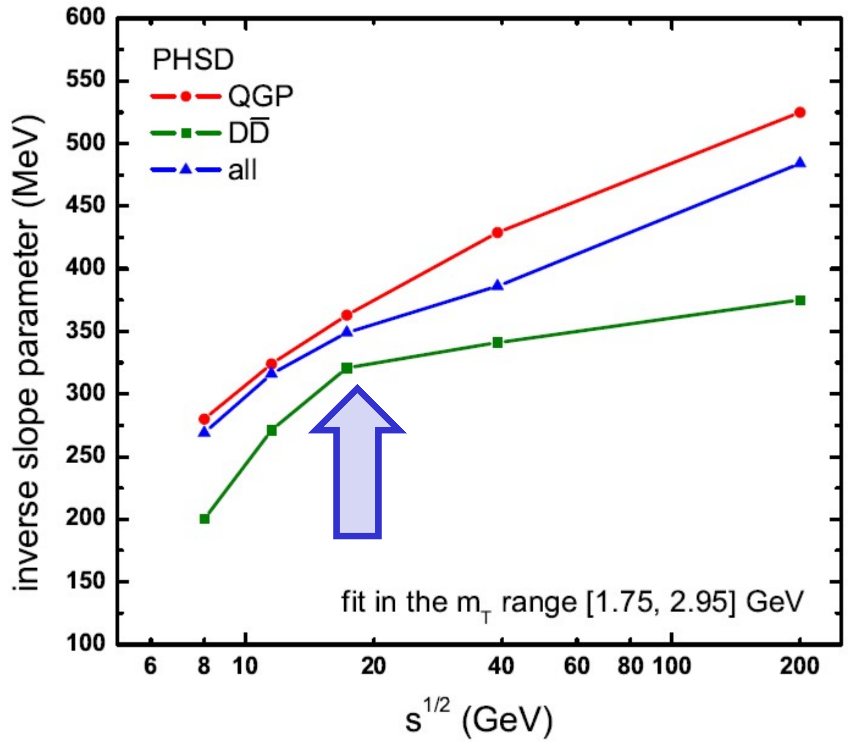

- **Inverse slope parameter: QGP contribution is harder than that from D-Dbar**
- **The excitation function of the total inverse slope parameter shows characteristic changes at $s^{1/2}$>20 GeV**

T. Song, W.Cassing, P.Moreau and E.Bratkovskaya, Phys. Rev. C 97 (2018) 064907

Messages from the dilepton study

❑ Low dilepton masses:

- Dilepton spectra show **sizeable changes due to the in-medium effects – modification of the properties of vector mesons** (as collisional broadening) – which are observed experimentally

- **In-medium effects** can be observed at **all energies from SIS to LHC; excess increasing with decreasing energy** due to a longer ρ-propagation in the high baryon-density phase

❑ Intermediate dilepton masses M>1.2 GeV :

- Dominant sources : **QGP** (qbar-q) , correlated charm D/Dbar

- Fraction of QGP **grows** with increasing energy; however, the relative contribution of QGP to dileptons from charm pairs increases with decreasing energy

➔ Good perspectives for **FAIR/NICA**

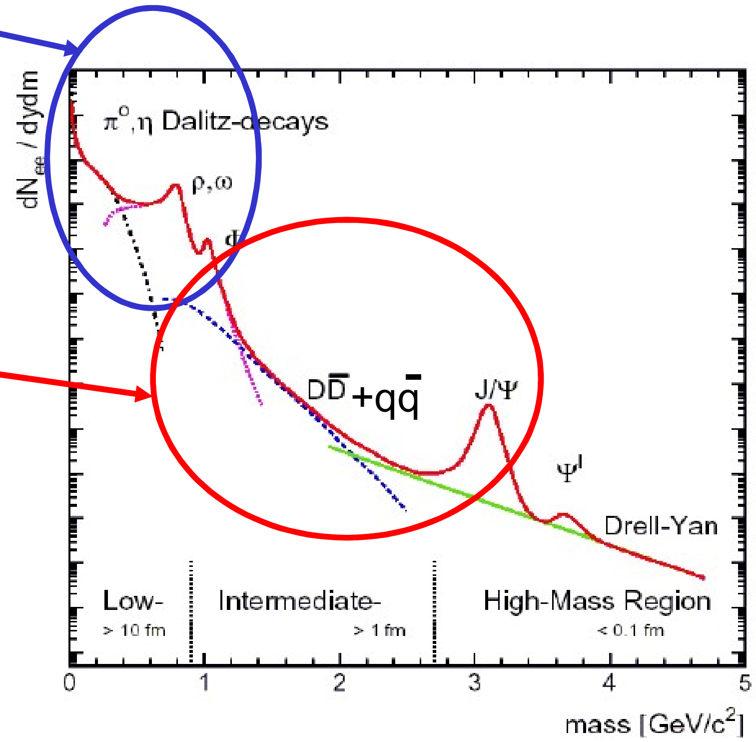

Review: O. Linnyk et al., Prog. Part. Nucl. Phys. 89 (2016) 50

T. Song, W.Cassing, P.Moreau and E.Bratkovskaya, Phys. Rev. C 97 (2018) 064907

Cluster and hypernuclei formation within PHQMD+FRIGA

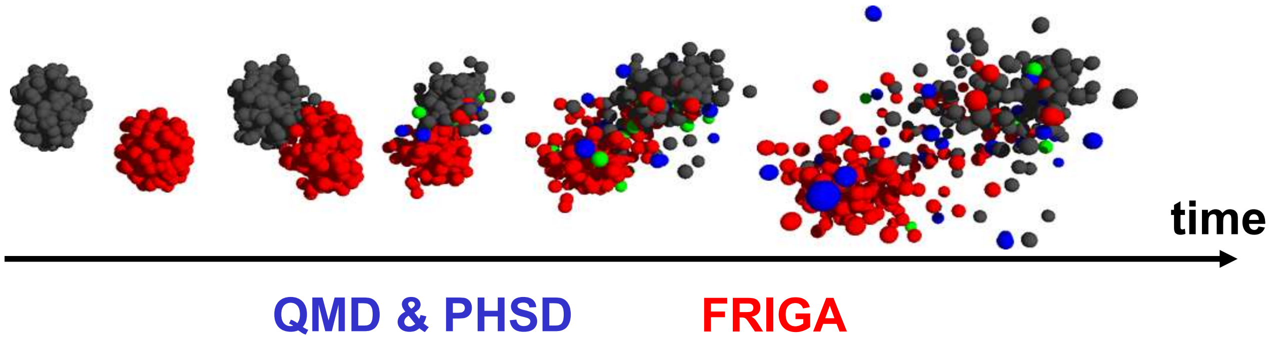

Clusters in HIC

At 3 AGeV, even in central collisions
20% of the baryons are in clusters,

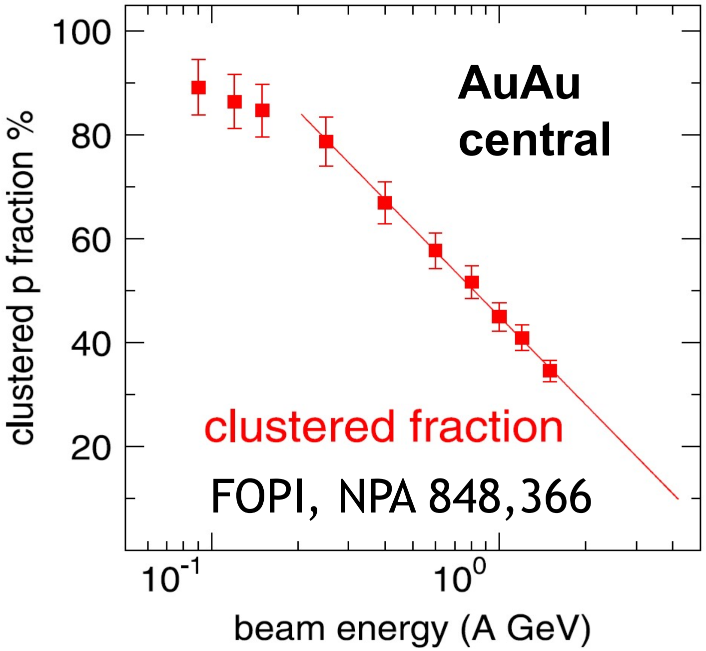

baryons in clusters have quite different properties (e.g. v_2):

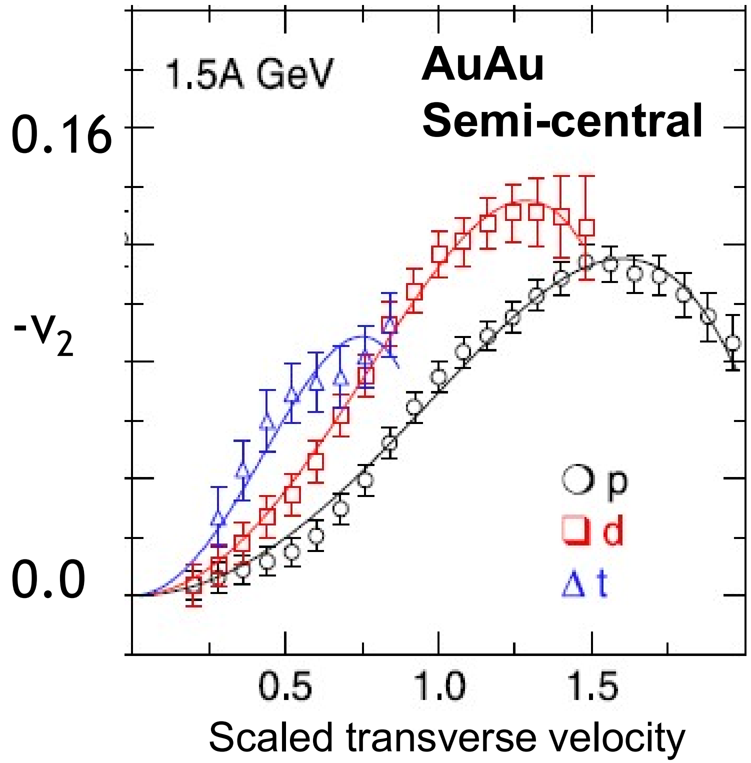

FOPI, NPA 876,1

Without dynamical formation of fragments

- **we cannot describe the nucleon observables (v_1 , v_2, dN/dp_T)**

- **we cannot explore the new physics opportunities like**
  hyper-nucleus formation
  1st order phase transition
  fragment formation at midrapidity

Modelling of fragment and hypernucleus formation

The goal: Dynamical modelling of cluster formation by a combined model
PHQMD = (QMD & PHSD) & SACA (FRIGA) *(presently under construction!)*

(GU & GSI & NANTES & JINR collaboration: E. Bratkovskaya, J. Aichelin, A. Le Fèvre, Y. Leifels, V. Kireev)

- **Parton-Hadron-Quantum-Molecular-Dynamics - a nonequilibrium microscopic transport model which describes n-body dynamics based on QMD propagation with collision integrals from PHSD (Parton-Hadron-String Dynamics) and cluster formation by the SACA model in comparison to the Minimum Spanning Tree model (MST). MST can determine clusters at the end of the reaction.**

- **Simulated Annealing Clusterization Algorithm – cluster selection according to the largest binding energy (extension of the SACA model -> FRIGA which includes hypernuclei). FRIGA allows to identify fragments very early during the reaction.**

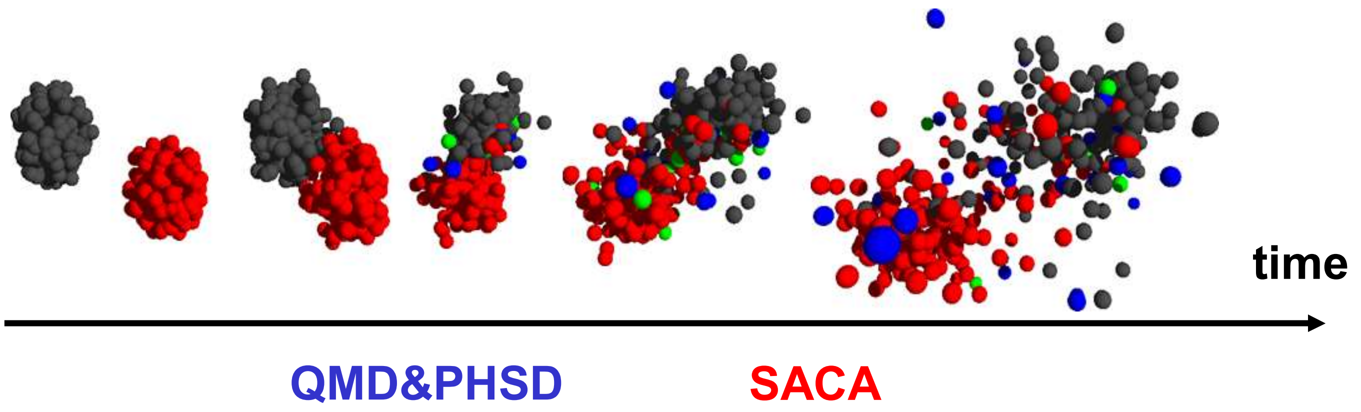

SACA: R. K. Puri, J. Aichelin, J.Comput.Phys. 162 (2000) 245-266
PHSD: W. Cassing, E. Bratkovskaya, PRC 78 (2008) 034919; NPA831 (2009) 215

Minimum Spanning Tree

The Minimum Spanning Tree (MST) is a cluster recognition method applicable for the (asymptotic) final states where coordinate space correlations may only survive for bound states.

The MST algorithm searches for accumulations of particles in coordinate space:

1. **Two particles are bound if their distance in coordinate space fulfills**

$$\left|\vec{r}_i - \vec{r}_j\right| \leq 2.5\, fm$$

2. A particle is bound to a cluster if it is bound with at least one particle of the cluster.

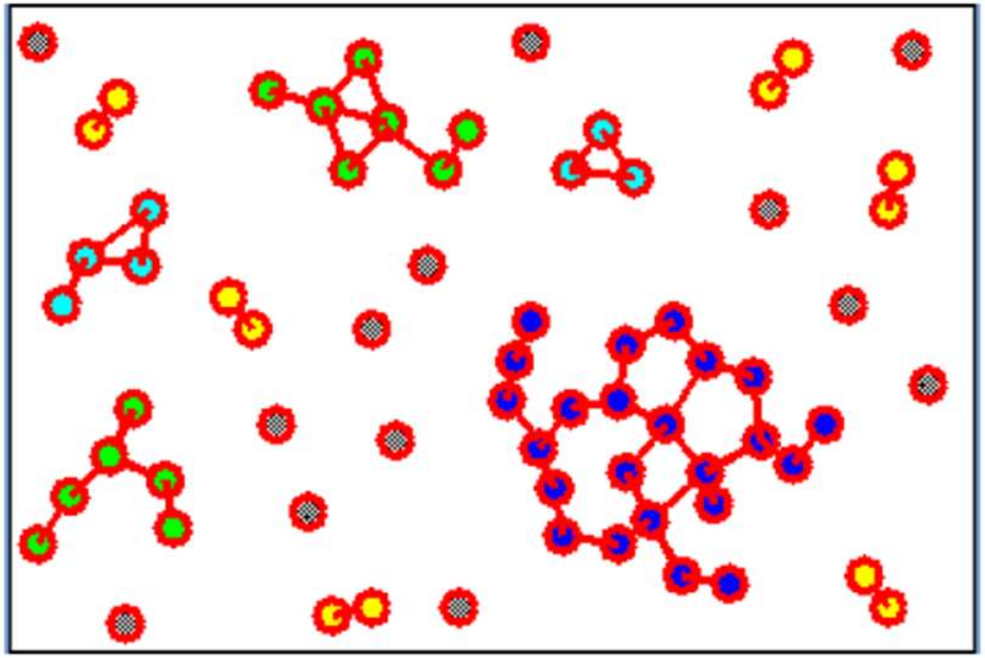

R. K. Puri, J. Aichelin, J.Comput.Phys. 162 (2000) 245-266

Simulated Annealing Clusterization Algorithm (SACA)

Take randomly 1 nucleon out of a fragment

Add it randomly to another fragment

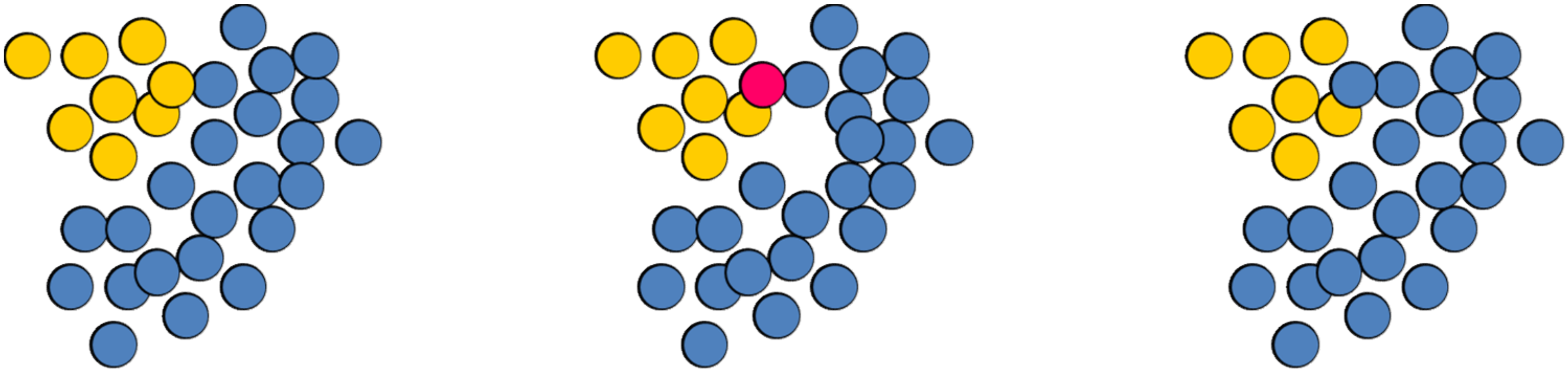

$$E=E^{1}_{kin}+E^{2}_{kin}+V^{1}+V^{2}$$

$$E'=E^{1'}_{kin}+E^{2'}_{kin}+V^{1'}+V^{2'}$$

If E' < E take a new configuration
If E' > E take the old configuration with a probability depending on E'-E
Repeat this procedure many times
→ Leads automatically to the most bound configuration

R. K. Puri, J. Aichelin, PLB301 (1993) 328, J.Comput.Phys. 162 (2000) 245-266;
P.B. Gossiaux, R. Puri, Ch. Hartnack, J. Aichelin, Nuclear Physics A 619 (1997) 379-390

‚Bulk' dynamics within PHQMD

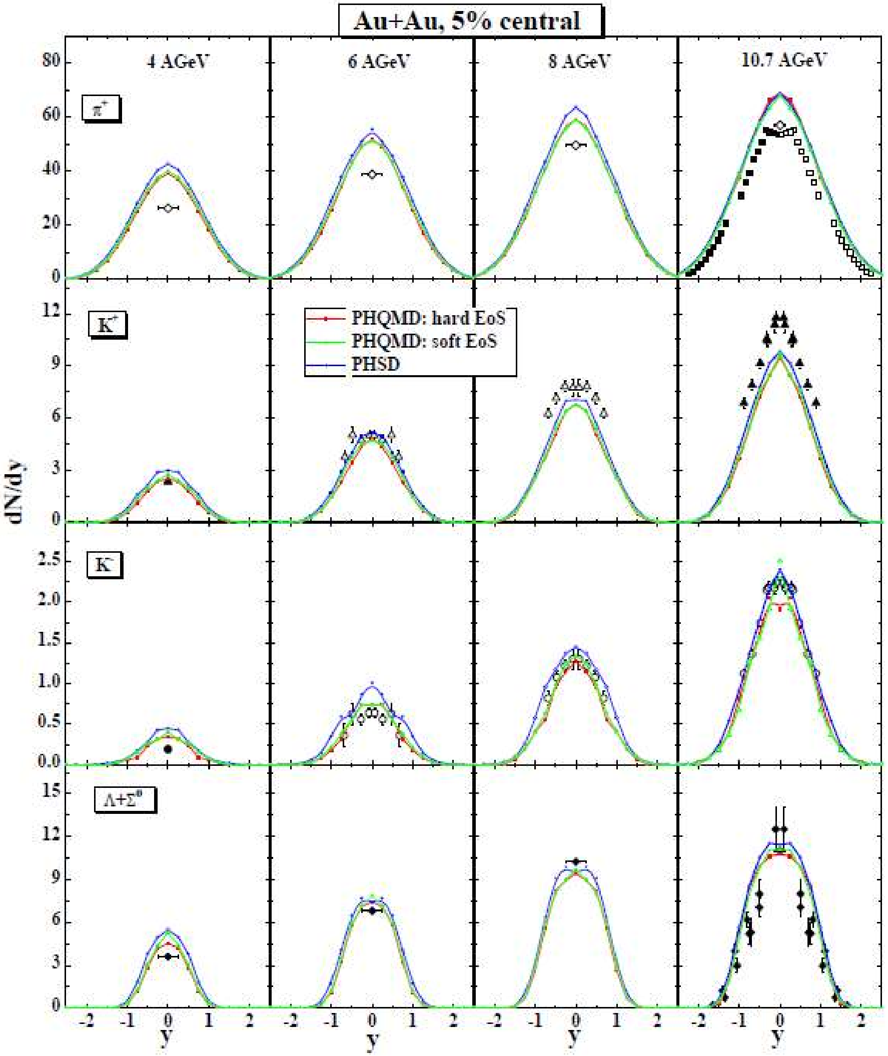

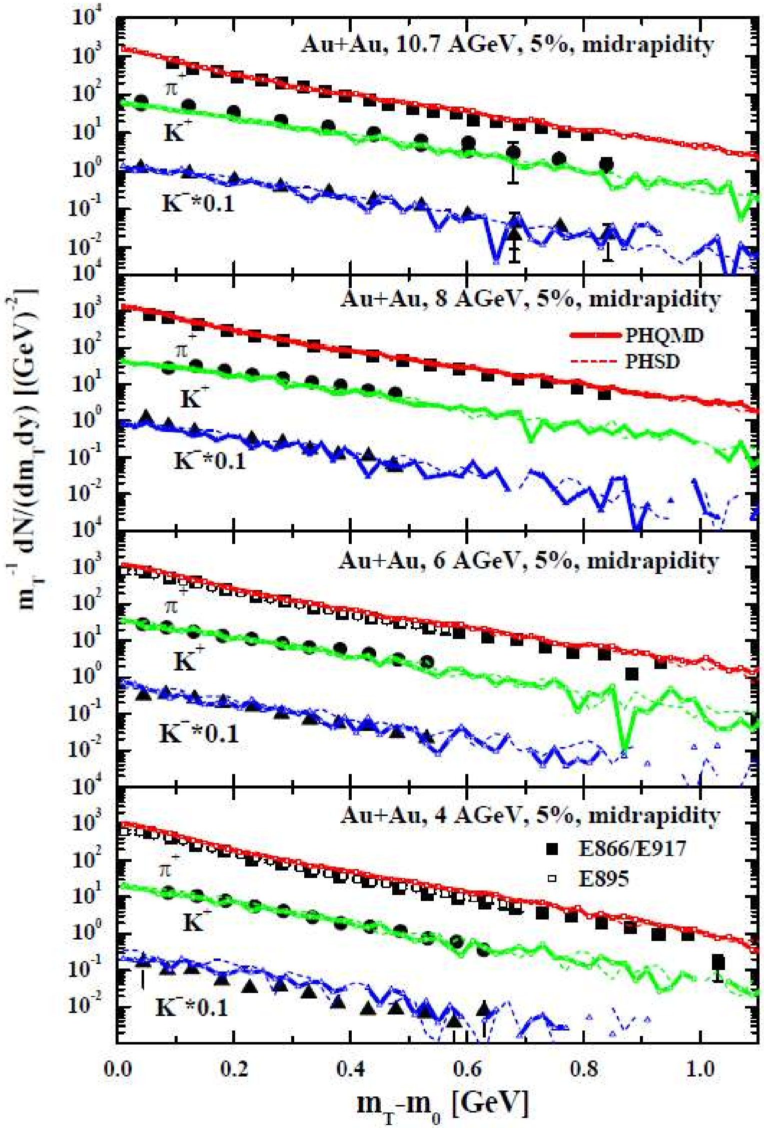

For newly produced particles:
PHQMD and PHSD give similar results – dominated by the collision integral from PHSD

Proton dynamics within PHQMD

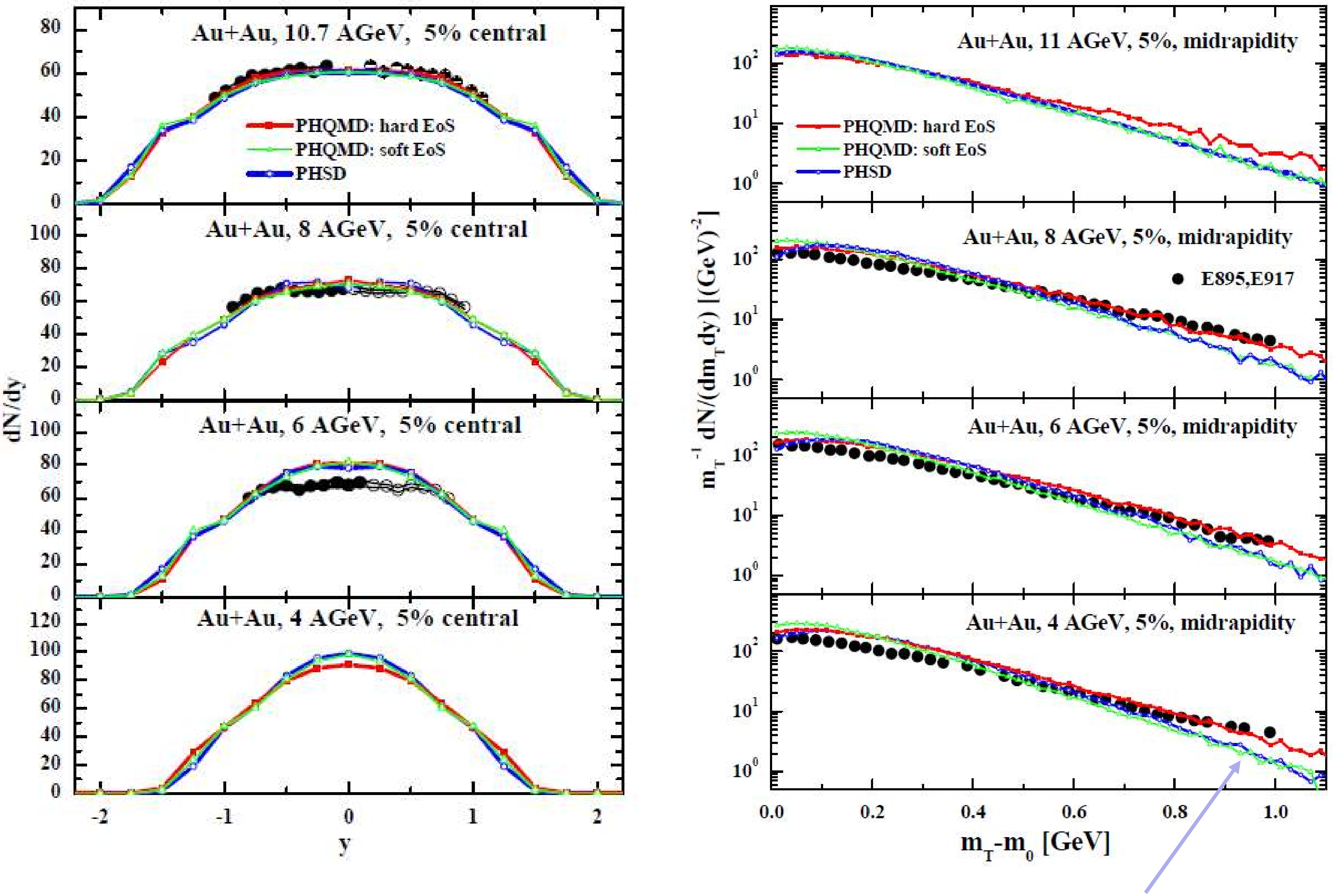

Proton spectra are sensitive to the nuclear potential (EoS)

Cluster formation within PHQMD

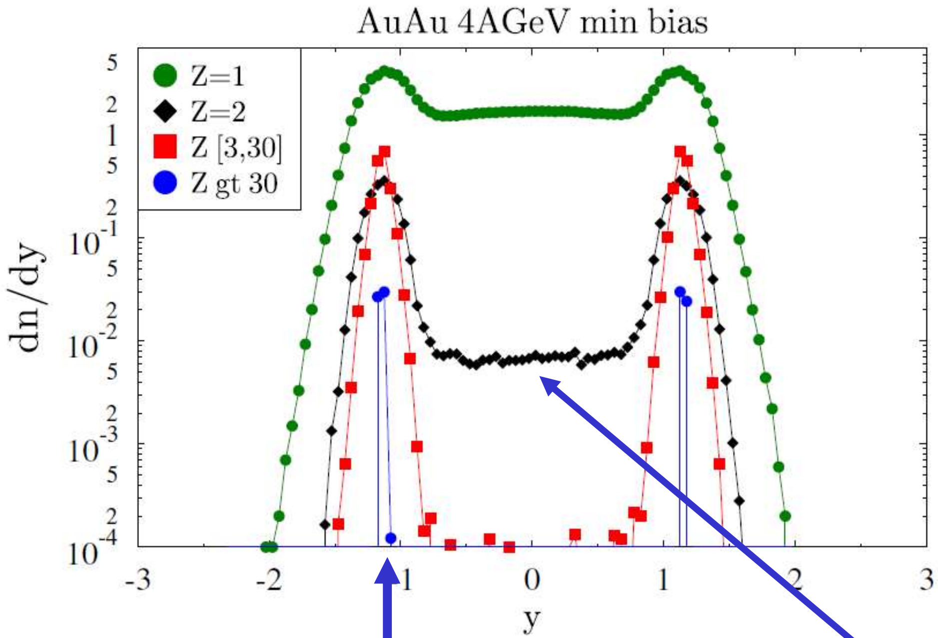

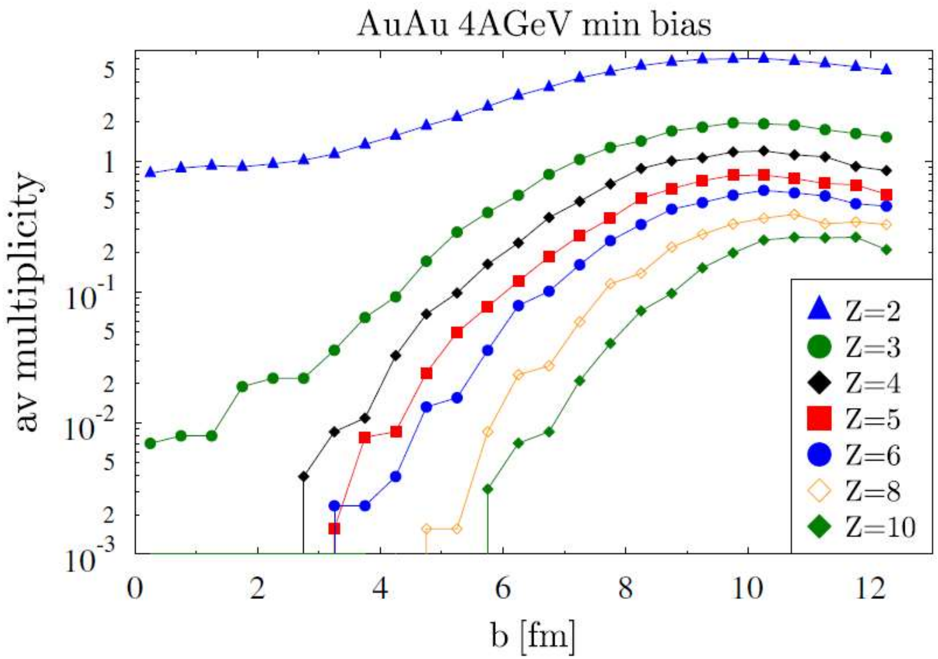

b dependence is non-trivial

There are two kinds of fragments

- **formed from spectator matter**
  close to beam and target rapidity
  initial-final state correlations
  heavy-ion reaction makes spectator matter unstable

- **formed from participant matter**
  created during the expansion of fireball :
  "ice" (E_{bind} ≈8 MeV/N) in
  "fire"(T ≥ 100MeV)
  *** seen from SIS to RHIC**

Cluster formation within PHQMD

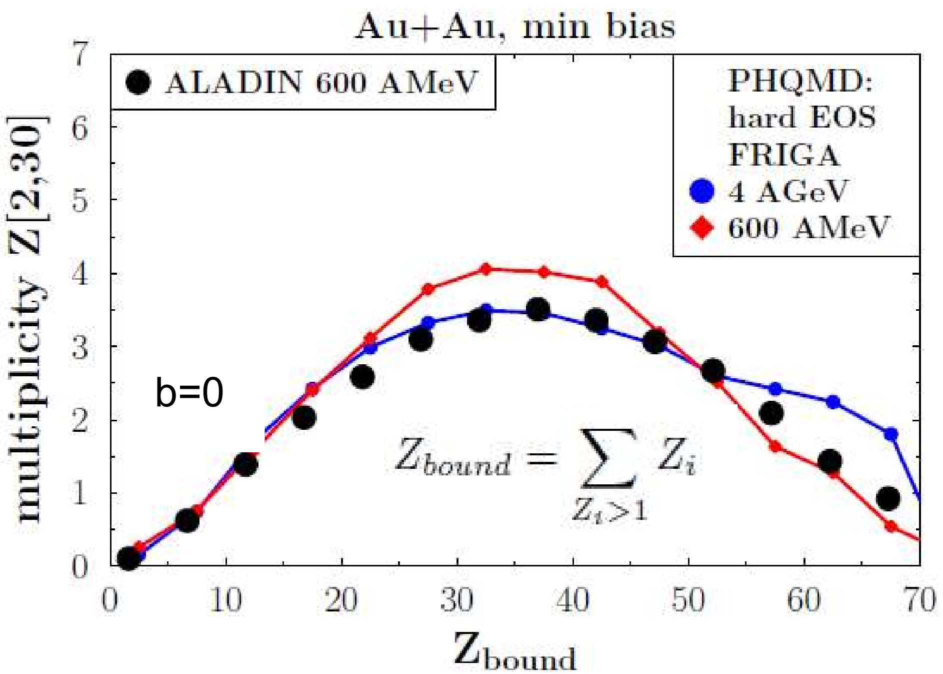

agreement for very complex fragment observables like the

- Energy independence of "rise and fall"
- Largest fragment (Z_{bound})

rms(p_t) shows $\sqrt{Z}$ dependence

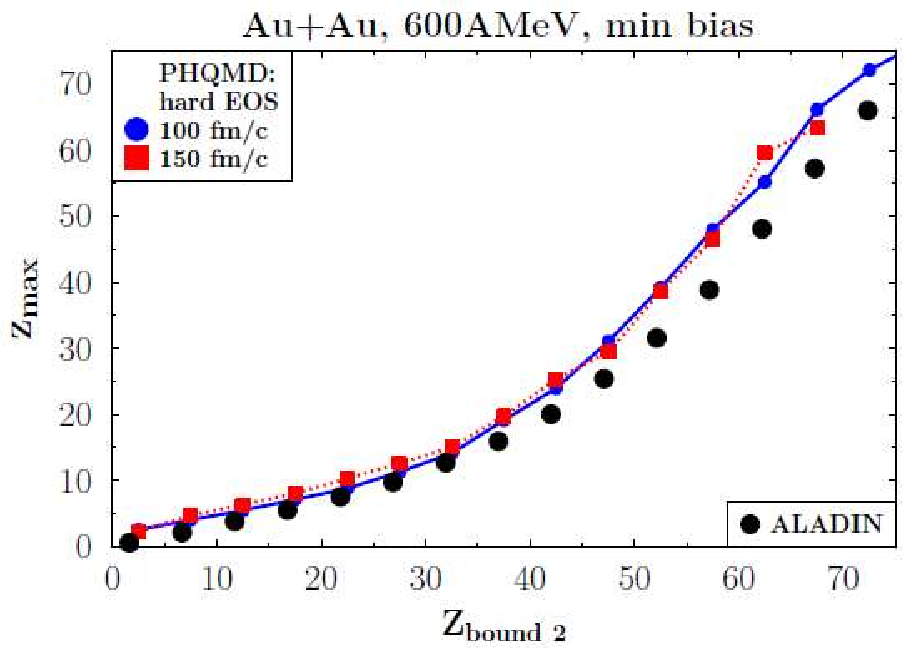

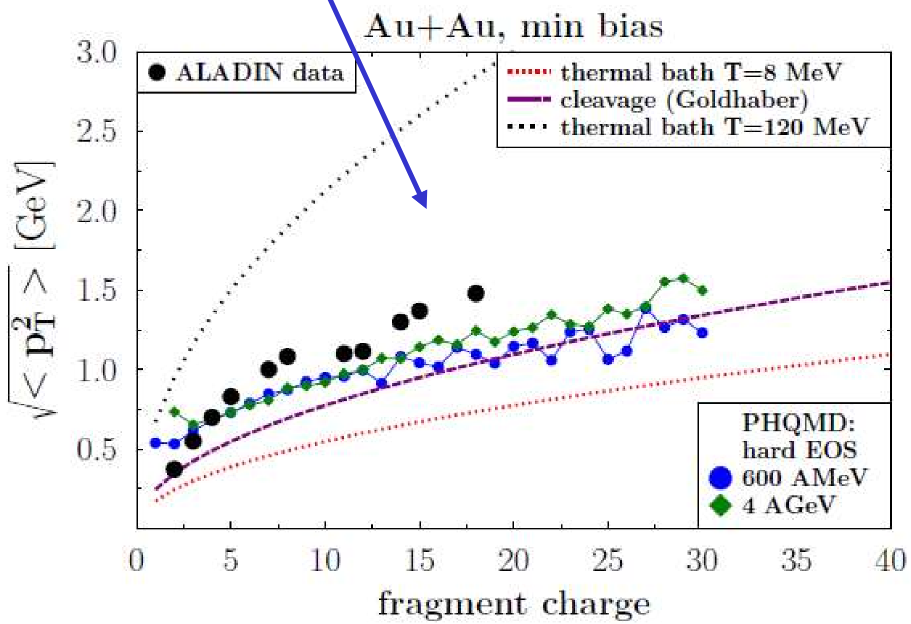

Hypernuclei formation within PHQMD

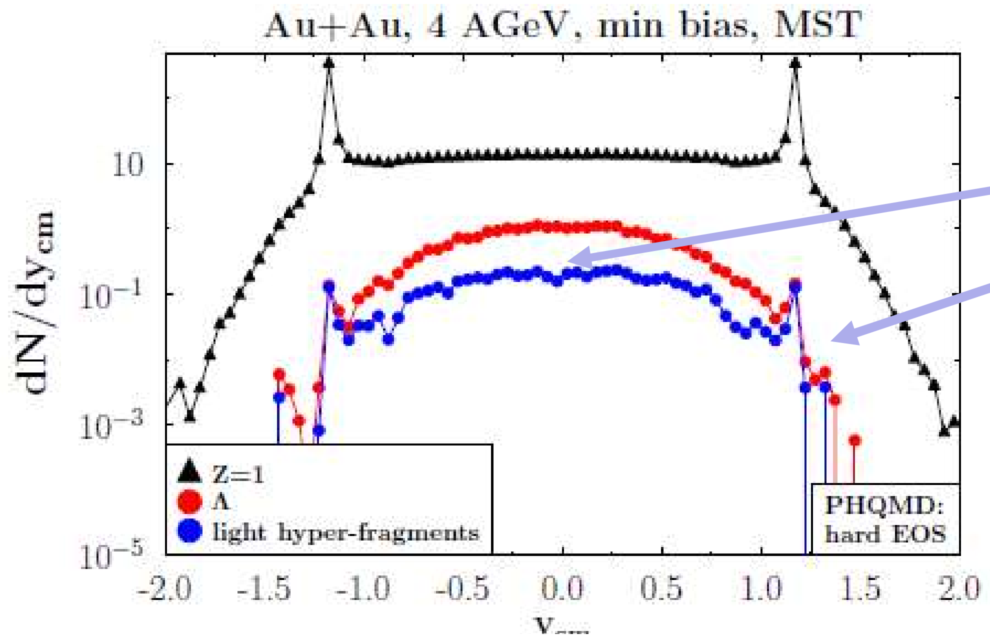

There are hypernuclei
- at midrapidity (small mass)
- at beam rapidity (large mass)

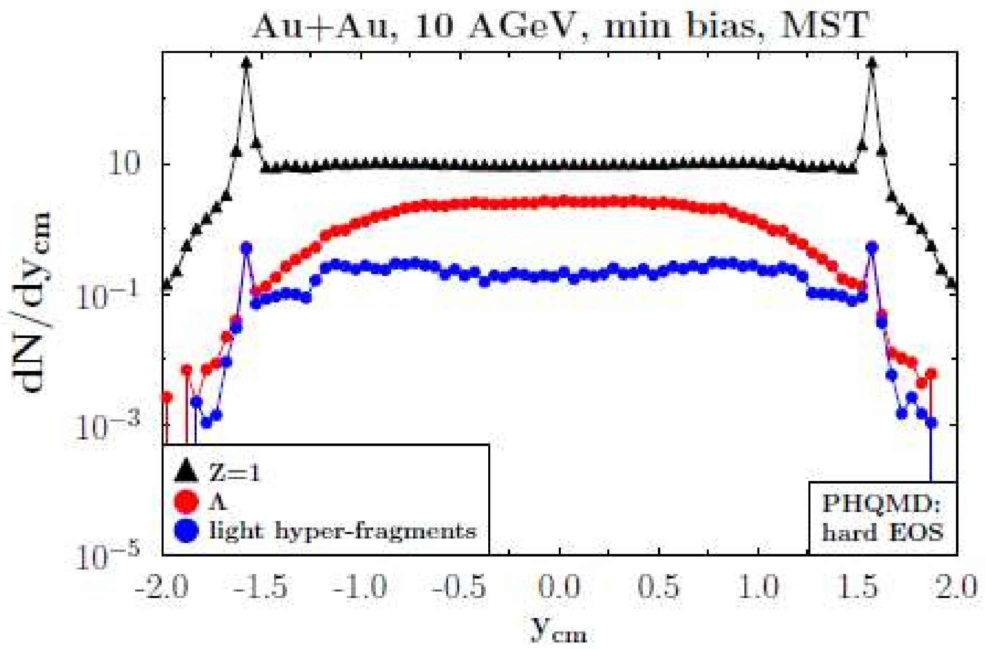

Central collisions → light hypernuclei

Peripheral collisions → heavy hypernuclei

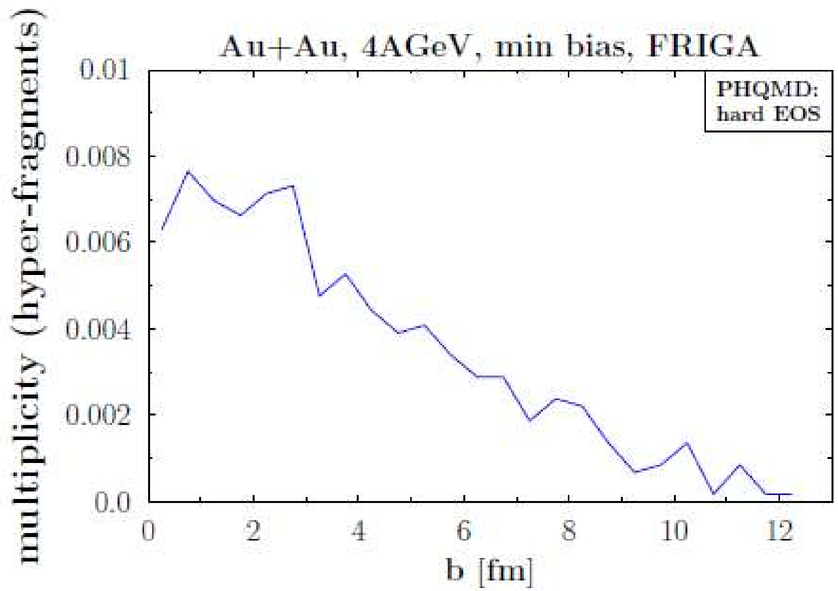

Summary: PHQMD

PHQMD provides a very good agreement with the presently available ALADIN fragment data as well as with the AGS/SPS single particle spectra

PHQMD allows

- to predict the dynamical formation of fragments
- to understand the proton spectra and the properties of light fragments (dN/dp_Tdy, v1,v2, fluctuations)
- to understand fragment formation in participant and spectator region
- to understand the formation of hypernuclei
- to study fragment formation at RHIC/LHC

Summary

Theory versus experimental observables:

- **indication for a partial chiral symmetry restoration**
- **evidence for strong partonic interactions in the early phase of relativistic heavy-ion reactions**

⇒ **formation of the sQGP in HIC!**

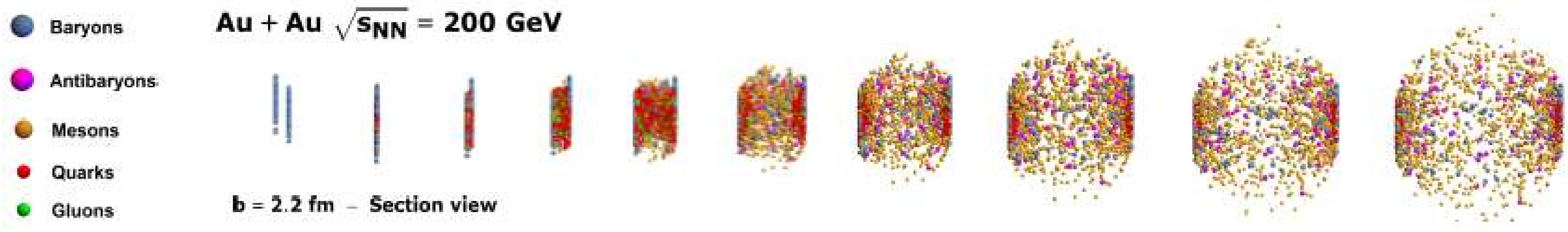

Thanks to: PHSD group - 2018

GSI & Frankfurt University
Elena Bratkovskaya
Pierre Moreau
Lucia Oliva
Olga Soloveva

Giessen University
Wolfgang Cassing
Taesoo Song

Thanks to Olena Linnyk
Volodya Konchakovski
Hamza Berrehrah

Thorsten Steinert
Alessia Palmese
Eduard Seifert

External Collaborations

SUBATECH, Nantes University:
Jörg Aichelin
Christoph Hartnack
Pol-Bernard Gossiaux
Marlene Nahrgang

Texas A&M University:
Che-Ming Ko

JINR, Dubna:
Viacheslav Toneev
Vadim Voronyuk
Viktor Kireev

Valencia University:
Daniel Cabrera

Barcelona University:
Laura Tolos

Duke University:
Steffen Bass

GSI
GOETHE UNIVERSITÄT FRANKFURT AM MAIN
FIAS Frankfurt Institute for Advanced Studies
HIC for FAIR Helmholtz International Center
HGS-HIRe for FAIR Helmholtz Graduate School for Hadron and Ion Research
Bundesministerium für Bildung und Forschung
DAAD
CRC-TR 211
DFG Deutsche Forschungsgemeinschaft
PHSD
JUSTUS-LIEBIG-UNIVERSITÄT GIESSEN
Subatech
TEXAS A&M UNIVERSITY
JINR
UAB Universitat Autònoma de Barcelona
Duke UNIVERSITY

Thank you for your attention !

Thanks to the Organizers !